NATIONAL ADVISORY COMMITTEE FOR AERONAUTICS

TECHNICAL NOTE 3042

HIGH-FREQUENCY PRESSURE INDICATORS FOR

AERODYNAMIC PROBLEMS

By Y. T. Li

Massachusetts Institute of Technology

NACA

Washington

November 1953

N

NATIONAL ADVISORY COMMITTEE FOR AERONAU.

TECHNICAL NOTE 3042

HIGH-FREQUENCY PRESSURE INDICATORS FOR

AERODYNAMIC PROBLEMS

By Y. T. Li
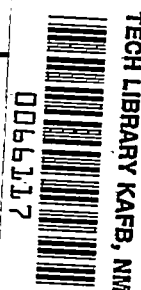
SUMMARY

Three different types of pressure indicators developed at the Massachusetts Institute of Technology are discussed in the present paper. Each of these indicators has a unique feature, but all are designed with an attempt to combine both high-frequency response and high resolving power into one instrument.

Of the mechanical-electrical-transducer type of pressure indicator, the wire strain gage leads in simplicity. The capacitance type is more versatile because it permits the use of very high frequency carrier systems and thereby cuts down the effective interference in the electronic system. The system utilizing the stretching of a barium-titanate disk produces large signals and results in compact design, but it can only be used for dynamic measurements when temperature variations are slight.

Five different types of pressure receivers, the cylinder, flat-diaphragm, spherical-diaphragm, catenary-diaphragm, and stretched-diaphragm or membrane types, were tested. The flat-diaphragm type leads the others in simplicity, the spherical-diaphragm type exceeds in dynamic performance, and the catenary-diaphragm type is the one least affected by temperature change.

The pressure indicators are dynamically calibrated by means of a shock tube.

INTRODUCTION

An important aspect of aerodynamic research is the determination of the gas pressure near the surface of an object in a flowing stream. Most often the pressure to be determined is of a static nature and its measurement can be done easily by pressure taps and manometers or similar instruments. However, there are numerous instances where the pressure to be determined is highly oscillatory because of disturbances in the stream or oscillatory motion of the body upon which the pressure is

measured. Examples of these are found in the operation of turbine or
compressor blades and in the phenomenon of flutter airfoils. When the
pressure of the stream is highly oscillatory its measurement becomes
more complicated and a simple pitot-tube type of arrangement is no longer
adequate because the response of this type of instrument is in general
too slow to give an accurate instantaneous account of rapidly changing
pressure. To get high response speed a pressure indicator utilizing a
system to produce an electrical output signal is generally used. But
even with an electrical output signal, which has the advantage of being
susceptible to amplification with practically no loss in response speed,
there is a certain limitation in frequency range for each type of configu-
ration. Furthermore, this limitation in frequency response is usually
lowered for a certain design when the instrument is required to give a
high resolving power. Design for indicators with both high-frequency
response and high resolving power is discussed in this paper. Some
previous investigations of this aspect of aerodynamic research are dis-
cussed in reference 1.

In addition to an adequate response speed and an acceptable resolving
power the pressure indicator which is suitable for aerodynamic research
must also incorporate the following considerations:

(1) Over-all size small enough to be mounted on the structural
member of the test body

(2) Diameter of pressure receiver smaller than the half wave length
of the pressure wave

(3) Insensitivity to vibration effects

(4) Insensitivity to environmental temperature change

(5) Adequate strength to withstand the possible application of a
certain maximum pressure without rupture

There is no single instrument which can embody all the requirements
for various types of applications. A practical design must concentrate
on the fulfillment of one or two requirements and sacrifice some other
criteria. For instance, in one case the over-all dimensions may be the
critical consideration while in another case exceptional high-frequency
response may be the determining criterion. In the present paper three
different types of pressure indicators developed in the Instrument
Laboratories of the Massachusetts Institute of Technology are discussed.
Each of these indicators has a certain unique feature but all are designed
with an attempt to combine both high-frequency response and high resolving
power into one instrument.

This investigation was conducted at the Massachusetts Institute of Technology and was financed in part by the National Advisory Committee for Aeronautics.

SYMBOLS

A effective area of pressure receiver

a_0 speed of sound in undisturbed gas

b width of diaphragm (see table I)

c_p specific heat at constant pressure

c_v specific heat at constant volume

E modulus of elasticity

e amplitude of dynamic error in deflection of pressure receiver divided by corresponding static deflection

h thickness of receiver

K elastic constant of pressure receiver

L length of compression chamber

l length of strain tube

m total mass of receiver

m_e effective mass of receiver

m_{eq} equivalent mass

n, n_r order integers of transient peaks

P resolving power

p_i interference equivalent pressure

p_0 expansion-chamber pressure

p_1 original shock-wave pressure

p_2 pressure in high-pressure chamber

p_3 reflected-wave pressure

S sensitivity of pressure receiver

T_r transient peak

$T_{n,nr}$ transient peak ratio

t_{p_3} time interval of reflected shock at pressure p_3

u independent variable

v dependent variable

y depth of spherical diaphragm

β frequency ratio

$\beta_p = \omega_p / \omega_n$

$\beta_{vib} = \omega_{vib} / \omega_n$

$\gamma = c_p / c_v$

δ deflection of pressure receiver due to vibration

δ_i interference displacement of pressure receiver

ϵ tension per unit length

ζ damping ratio

$\eta = (\gamma + 1)/(\gamma - 1)$

λ speed of sound in receiver material

μ amplitude ratio

ξ pressure ratio of normal shock, p_0/p_1

ξ' pressure ratio of reflected shock, p_1/p_3

ρ density

σ_{max} maximum allowable stress

τ low-damping-ratio characteristic time

ψ dynamic response angle

ω_n natural undamped frequency of pressure receiver

ω_p frequency of pressure fluctuation

ω_{vib} frequency of vibration

Subscripts:

c   pertains to compression chamber

e   pertains to expansion chamber

DESIGN PRINCIPLES FOR PRESSURE RECEIVERS

Pressure indicators suitable for high-frequency applications invariably utilize a mechanical pressure receiver as the basic measuring element. The essential functions of this receiver are to provide a seal and an elastic restraint. The pressure acting over the area of the seal produces an actuating force. The corresponding elastic deflection is the useful output of the pressure receiver. Conversion of the deflection to an electrical signal is a convenient means for producing an indication since such a signal may be readily amplified. Also electrical measurements are well suited for high-frequency operation. In fact, when electrical deflection measurement is employed, the dynamics of the pressure receiver determine the upper frequency range of the pressure indicator.

A mechanical pressure receiver is characterized by its sensitivity and its natural modes of vibration. The sensitivity is defined as the ratio of the deflection of the receiver to the corresponding applied pressure. Ideally, this sensitivity is constant over the entire pressure range and any environmental operating condition. Its minimum value is established by the requirement that the indicator resolve clearly some specified threshold pressure change. The characteristics of the transducer, amplifier, and indicator as well as consideration of interference effects are all involved in this determination. As for the natural modes of vibration, the fundamental or lowest frequency mode is most important. This natural frequency limits the frequency range over which pressure measurements can be made without introducing objectionable dynamic error. Further, if the pressure receiver is subjected to mechanical vibration as an interfering input, undesirable spurious signals are produced, which increase with the vibration frequency when this frequency is less than the natural frequency. Because of these effects, the natural frequency of the pressure receiver must be considerably higher than both the

highest frequency pressure fluctuation being measured and the highest
mechanical-vibration frequency which is present.

When the pressure-fluctuation frequency or vibration frequency is
small in comparison with the receiver natural frequency, the dynamic
error associated with pressure fluctuations

$$e \approx \beta_p{}^2 \qquad\qquad (1)$$

and for the interfering effect of mechanical vibration

$$\delta \approx \mu_{vib}\beta_{vib}{}^2 \qquad\qquad (2)$$

where

e amplitude of dynamic error in deflection of pressure receiver
divided by corresponding static deflection

δ deflection of pressure receiver due to vibration

μ_{vib} amplitude of mechanical vibration

β_p frequency of pressure fluctuation divided by natural undamped
frequency of pressure receiver, ω_p/ω_n

β_{vib} frequency of vibration divided by natural undamped frequency
of pressure receiver, ω_{vib}/ω_n

For practical purposes, a pressure receiver may be represented by a
mechanical system having a certain elastic coefficient and equivalent
mass, the ratio of which determines the undamped circular natural frequency:

$$\omega_n{}^2 = \frac{K}{m_{eq}}$$

The elastic constant and the effective area A of the pressure
receiver determine the sensitivity

$$S = \frac{A}{K}$$

Thus, the natural frequency may be written

$$\omega_n{}^2 = \frac{A}{S m_{eq}} \tag{3}$$

Equation (3) shows that the natural frequency can be increased by decreasing the sensitivity or the effective mass per unit area of the receiver.

Increase of natural frequency by reduction in sensitivity is accompanied by a reduction in resolving power of the indicator. Resolving power is defined as the reciprocal of the smallest pressure change detectable by the indicator. Resolving power is determined with regard to the levels of various interfering inputs which may appear at the pressure receiver, transducer, and amplifier. The effects of such interfering inputs may be compared if they are all referred back to an equivalent pressure at the pressure receiver. Generally speaking, this interference equivalent pressure may not be greater than the desired smallest measurable pressure change. Thus, it is reasonable and convenient to equate these quantities in order to arrive at a useful design criterion. For an interference displacement of the pressure receiver, designated by δ_i, the corresponding interference equivalent pressure p_i will be δ_i/S. The resolving power is then

$$P = \frac{1}{p_i} = \frac{S}{\delta_i} \tag{4}$$

If equations (1), (3), and (4) are combined, the result is

$$\frac{m_{eq}}{A} \equiv \frac{e}{\delta_i \omega_p{}^2 P} \tag{5}$$

If the interference displacement is caused by pressure-receiver vibration, equation (5) becomes

$$\frac{m_{eq}}{A} \frac{1}{\omega_n{}^2} = \frac{e}{P a \omega_{vib}{}^2 \omega_p{}^2} \tag{6}$$

Equations (5) and (6) are arranged to show that for a given interference level and a given pressure frequency, the mass per unit area is determined

by the desired resolving power and the tolerable dynamic error. Thus
the mass per unit area of the pressure receiver is a basic criterion for
design purposes. The importance of this design parameter becomes con-
trolling at high frequencies. As an example, assume that a flat steel
diaphragm indicator is required to resolve a pressure of 0.1 pound per
square inch at a frequency of 10,000 cycles per second with an allowable
dynamic error of 20 percent in the presence of interferences which cause
a diaphragm deflection of 0.0001 inch. Substitution of these values in
equation (5) gives mass per unit area corresponding to 0.0001 inch for a
resulting diaphragm thickness, an impractically thin diaphragm for serv-
ice use. Clearly, efforts toward improving high-frequency performance
must include minimization of the mass per unit area of the pressure
receiver consistent with manufacturing and service flexibility. Such
efforts must also include minimization of interference effects. Schemes
for accomplishing this are discussed below in connection with actual
indicator designs.

The foregoing analysis becomes inaccurate when β_p or β_{vib} is
greater than 0.2 or 0.3. Accordingly, for these results to apply, pres-
sure frequencies must be well below the receiver natural frequency. Fur-
ther in connection with vibration interference, as shown in equation (6),
higher natural frequency makes possible higher mass per unit area for the
same resolving power and dynamic-error tolerance, although it should not
be inferred that natural frequency and mass per unit area are unrelated.
Thus natural frequency in addition to mass per unit area plays a critical
role in the high-frequency performance of pressure receivers.

CHARACTERISTICS OF FIVE TYPES OF PRESSURE RECEIVERS

Table I lists the characteristics of five different types of pressure
receivers which may be used for high-frequency measurements. Included in
the listing are natural frequency, sensitivity, ratio of effective mass to
true mass, and maximum allowable pressure. The ratio of effective mass to
true mass is that fraction of the total diaphragm mass which is effective
in determining the natural frequency. The quantities listed in table I
are nondimensionalized in order to facilitate type comparisons.

The cylindrical type of pressure receiver is not suitable for high-
frequency pressure measurements in gases because it introduces an acous-
tical cavity which causes additional dynamic error. It is otherwise ade-
quate and is included in the table.

Of all types of pressure receivers, the flat-diaphragm type is the
most simple and most easily adapted for flush mounting. Increasing the
diaphragm thickness increases the natural frequency but unfortunately
also increases the parameter of mass per unit area. For this reason a
flat diaphragm used for high-frequency applications is limited in resolving
power.

The third type of pressure receiver consists of a diaphragm which is a section of a spherical shell. The natural frequency of such a pressure receiver depends upon its depth ratio just as that of a flat diaphragm depends upon its thickness ratio. At 50,000 cycles per second the required depth ratio is about 1/20 for a steel diaphragm of 1/2-inch diameter. This is sufficiently shallow so that it may be considered to be flush mounted for most practical purposes. In this type of receiver, the natural frequency is independent of the diaphragm thickness which means that the mass per unit area can be reduced by making the diaphragm thinner, thus increasing sensitivity without sacrificing dynamic error. Further, for the spherical diaphragm, the ratio of effective mass to true mass is about one-fourth of that for the flat diaphragm. Also because of the spherical shape, the spherical diaphragm will withstand 12 times the allowable pressure which may be applied to the comparable flat diaphragm.

In certain transducers, diaphragm motion varies a gap to the length of which the sensitivity is inversely proportional. If diaphragm motion is a linear function of pressure, the transducer output will be nonlinear with pressure. As shown in table I, the spherical diaphragm motion in response to pressure is inversely proportional to the square of diaphragm depth. This effect tends to compensate for transducer nonlinearity, particularly for shallow diaphragms which are used when higher sensitivity is required.

Like the spherical diaphragm, the catenary type is characterized by the efficient use of structural material to achieve high performance. Its natural frequency depends primarily upon the length of the supporting tube. Its effective-mass ratio is rather high because of the use of a supporting tube in addition to the diaphragm. But it can outperform the flat diaphragm over a wide range of applications because its natural frequency is independent of diaphragm thickness. The outstanding feature of this type of pressure receiver is that its elastic member is separated from the seal. In the four other types described each is constructed with a single element which serves both as the seal and the elastic element. Under that condition the elastic element is necessarily in direct contact with the medium the pressure of which is being measured, and so partakes of the temperature changes of the medium. In the catenary-diaphragm-type pressure receiver, the supporting tube acts as the principal elastic restraining member. It is not in close thermal contact with the environment and consequently is subject to less interference due to temperature.

In the stretched-diaphragm type of pressure receiver, the diaphragm is so thin that it cannot sustain bending moments and hence is treated as a membrane. The natural frequency of this type depends entirely on the initial tension in the diaphragm. Thus the upper limit on natural frequency is set by the allowable stress in the diaphragm material. For example, if the maximum allowable diaphragm stress is 150,000 pounds per square inch, the natural frequency is less than one-fifth of the natural

frequency attainable in the other types under discussion. Nevertheless a membrane can have a natural frequency greater than that of a flat diaphragm of the same thickness. With regard to mass per unit area, the stretched membrane is comparable with the spherical diaphragm. These two types have comparable performance except that the membrane type is restricted to lower frequencies. Also the allowable pressure for a membrane decreases with increasing natural frequency. Finally, the membrane is very susceptible to temperature changes since such changes alter the diaphragm tension and hence the sensitivity.

In summary, the following general remarks may be made about the foregoing types of pressure receivers. The flat-diaphragm type leads the others in simplicity. The spherical-diaphragm type excels in dynamic performance. The catenary-diaphragm design is least affected by temperature changes. In the following sections, the designs of pressure indicators based on these principles are described.

SPHERICAL-DIAPHRAGM INDICATOR WITH CAPACITIVE TRANSDUCER

Since the spherical-diaphragm type of pressure receiver has the best dynamic characteristics, it is well suited for very high frequency pressure measurements such as are associated with the operation of high-speed turbine blades. In figure 1 the sensitivity of such a pressure receiver is compared with that of a flat-diaphragm type which has hitherto been commonly used for this purpose. In the high-frequency range the advantage in using the spherical diaphragm design is obvious; for example, at 100,000 cycles per second the sensitivity of the spherical diaphragm is about 50 times as great as that of the flat diaphragm. Figure 1 is based on steel diaphragms 0.001 inch thick. In the spherical shape this is a perfectly reasonable thickness. In fact, if greater sensitivity is required it is quite feasible to make a spherical diaphragm as thin as 0.00025 inch.

Figures 2 and 3 show a spherical-diaphragm type of indicator having a variable-capacity transducer. In the model constructed a 5/16-inch-diameter diaphragm is the ground electrode. The fixed electrode is spherically shaped to match the curvature of the diaphragm and is spaced with a 0.002-inch normal air gap. Diaphragm deflection due to pressure changes the capacity of the air gap, which is detected by means of high-frequency circuitry utilizing either frequency modulation or amplitude modulation. The associated electronic equipment which was used is of the design of the General Motors Research Corporation employing a tuned circuit of 400 kilocycles per second (ref. 2). The static calibration curve for this indicator is shown in figure 4. Other characteristics are listed in table II.

HIGH-RESOLVING-POWER PRESSURE INDICATOR

WITH STRAIN-GAGE TRANSDUCER

A pressure indicator employing a catenary diaphragm and strain-gage transducer was described by Draper and Li (ref. 1). This indicator has outstanding over-all performance and in particular its susceptibility to temperature change is very small. For this reason it is particularly useful in pressure measurements associated with various types of power plants. The construction of the original indicator is shown in figure 5 in which the catenary diaphragm is supported by a strain tube. Two strain-gage windings are bonded to the surface of the tube in order to measure the change in strain of the tube when pressure is applied to the diaphragm. The principal reason for the excellent temperature behavior of this indicator is that the strain tube represents the major part of the total elastic restraint and is protected from large environmental temperature changes by a supply of cooling air. This maintains the elasticity constant and hence the sensitivity nearly constant. Also, since the diaphragm is much more flexible than the strain tube, differential thermal-expansion effects for various parts of the indicator are greatly reduced. And finally, with respect to the transducer, the use of two strain-gage windings in close thermal contact and connected as adjacent bridge arms largely elimates temperature effect. The natural frequency of the indicator is greater than 45,000 cycles per second and may be increased if necessary to 100,000 cycles per second.

The original indicator as shown in figure 5 is inadequate for low-pressure measurements. The resolving power, determined by amplifier noise, is no better than 1/2 pound per square inch when a steel strain tube is used with a 1/2-inch diaphragm. This may be reduced to about 1/4 pound per square inch by use of an aluminum-alloy strain tube, but even this is inadequate for use in connection with low-pressure fluctuations. For this reason the original design was modified.

Figures 6 and 7 show a catenary-diaphragm strain-gage pressure receiver for low-pressure use. This indicator retains most of the high-frequency performance of the original design but has increased resolving power by a factor of 10. In this design the strain tube is omitted and replaced by an unbonded strain gage formed in the shape of a ribbon with two windings. A longitudinal winding serves as the pressure-measuring gage and a transverse winding is used for temperature compensation. The longitudinal winding is attached to the diaphragm by means of a U-shaped hook.

With a diaphragm thickness of the order of 0.0005 to 0.001 inch, the diaphragm stiffness is too low to maintain tension in the longitudinal strain gage or to withstand pressure applied to the diaphragm. For this

reason, a back pressure of about 40 pounds per square inch is maintained behind the diaphragm. This back pressure maintains the longitudinal strain gage winding under high initial tension, which is reduced as pressure is applied to the diaphragm. In applications where high-frequency performance is less critical, a heavier diaphragm may be used. If a diaphragm thickness of 0.003 inch is used the diaphragm becomes sufficiently strong to make unnecessary the use of back pressure. In this instance, however, the diaphragm contributes part of the elastic restraint of the pressure receiver, which increases the sensitivity of the indicator to temperature.

Static calibration curves for a 5/16-inch-diameter indicator and for a 1/2-inch indicator are shown in figure 8. These are both of the thin-diaphragm type with back pressure. Other characteristics of these indicators and of a stiffer diaphragm type are given in table III.

MINIATURE PRESSURE PICKUP WITH BARIUM-TITANATE TRANSDUCER

In the measurement of varying pressures associated with a high-speed wind-tunnel model, the primary requirement placed on the pickup element is that it be of small size and flush-mounted. Also of major importance is a moderately high natural frequency so as to render it insensitive to acceleration effects.

To fulfill these requirements a circular pressure pickup with the diameter ranging from 5/16 to 1/2 inch and a thickness of less than 3/32 inch was developed. Figure 9 shows the construction of this unit. The pickup consists of a metal case with a flat diaphragm as an integral part. A disk of barium titanate is mounted on the inner surface of the diaphragm, such that when pressure is applied to the diaphragm causing it to deflect, the ceramic sheet is stretched. When properly polarized, the ceramic element exhibits a pronounced piezoelectric phenomenon and produces a charge across the surfaces of the sheet. An electrode on each surface collects the charge and gives an electrical output signal corresponding to the strain produced in the ceramic by the pressure.

The general arrangement of the button-sized pressure indicator is shown by figure 10. Installation of this unit into a seat of a model is achieved with the use of a corrugated steel ribbon. The seat is slightly larger than the pickup, so that an annular gap is maintained between them. The ribbon is then fitted into the gap. Because of its corrugation a certain amount of radial force is created around the gap to provide enough friction to hold the pickup in place. In addition to this some wax may be used to smear around the gap to improve the seal and provide necessary fairing.

The performance of the button-sized indicator is summarized in table IV.

A pressure pickup of this design can produce large electrical signals without excitation. Using a vacuum-tube voltmeter, 200 millivolts of output per pound per square inch of pressure can be obtained. This device has, however, two major drawbacks: Extreme sensitivity to temperature changes and poor low-frequency response. The latter difficulty is due to current leakage through the capacitance of the pickup or the input stage of the indicating system. To overcome these difficulties two schemes are adopted as described below.

Temperature Compensation

Figure 11 shows an exaggerated sectional view of the diaphragm-ceramic assembly under pressure. The diaphragm modulus of elasticity is approximately four times higher than that of the ceramic and therefore carries a larger share of the load. This results in the deflection of the assembly being primarily determined by the characteristics of the metal diaphragm. The diaphragm is an integral part of the rim which is relatively rigid so that the diaphragm behaves as a diaphragm with clamped edge. When deflected, the center portion of the lower surface of the diaphragm is in tension and the area near the rim is in compression as shown in the figure. To utilize this difference in strain the electrode on the ceramic is divided into two concentric sections and the sections polarized with opposite orientation. Since the strain is also of opposite sign, the charges collected on each section of the electrode are of the same sign when a pressure is applied to the diaphragm. However, when a change in temperature is introduced, the charge produced in each section would be of opposite sign because of the reversed orientation. Proper apportioning of the section areas results in a gain of about 50 percent in pressure signal and a reduction by a factor of 10 in temperature effect over that obtained for the undivided-electrode type.

Low-Frequency-Response Compensation

The poor low-frequency response of the barium-titanate pressure pickup is because of the leakage of the ceramic element and the input stage of the amplifier. In general, leakage is associated with a potential difference. For this reason, if the charge is removed from the ceramic element as soon as it is produced to allow no voltage buildup, there shall be no leakage. Using this principle, a circuit with a feedback loop is constructed as shown in the schematic diagram of figure 12 (see ref. 3). Assuming that the gain of the amplifier is infinite, then the input of this amplifier is not changeable with the feedback effect of condenser c_2. Under these circumstances any charge produced by

condenser c_1 would be transferred to condenser c_2. Condenser c_2 is
a high-quality condenser with a very low leakage. When a charge is trans-
ferred to condenser c_2 there is a corresponding change of potential at
the output stage of the amplifier. This output voltage becomes the sig-
nal of the pressure indicator.

Figure 13 shows the circuit for performing the function described
in the schematic diagram of figure 12. The amplifier of this circuit
consists of one single-stage amplifier and a cathode follower. The
cathode of the amplifier is tied to the cathode of the cathode follower
to achieve a regenerative feedback. By proper adjusting of the regener-
ative circuit, the gain of the amplifier can be boosted far beyond the
gain of a two-stage amplifier. In the present arrangement with only two
tubes, it combines the three desired features such as (1) a high gain,
(2) an inverse amplification, and (3) a low output impedance.

Under ideal operating condition a scheme as shown in figures 12
and 13 should not receive any electrical charge at the input except that
from the pickup. In practice, however, stray charges may be received
from sources other than the pickup from time to time. The largest source
of stray charges comes from the input grid of the amplifier. If the grid
has sufficient negative bias, this undesirable flow of charge may be
reduced considerably. Stabilization of the heater voltage also helps to
bring down the drifting effect due to grid leakage. To remove the last
bit of drift a sacrifice of the direct-current response is necessary.
In the circuit of figure 13 a resistor of 100 megacycles is used to clamp
the output signal with respect to the input. When this resistor is
brought into the circuit the frequency response shows a decline below
$1/2$ cycle per second; but the average output level becomes quite stable.
The sensitivity of the system, within the flat-frequency-response range,
is not affected by the use of this resistor. For this reason it is possi-
ble to make static calibration without the resistor and make dynamic meas-
urement with the resistor in the circuit. The output bias voltage pro-
vided by the battery and potential meter shown in the circuit of figure 13
is used to bring the output level equal to ground level so that the on-off
action of the resistor would not disturb the stable condition of the cir-
cuit and at the same time permit an easy hookup with an indicating system.

DYNAMIC CALIBRATION OF PRESSURE INDICATORS BY MEANS OF SHOCK TUBE

Generally speaking, the dynamic performance of a pressure indicator
can be represented by an equivalent second-order system. Such a system
is characterized by frequency-response curves showing amplitude and phase
angle or by the numerical values of the two dynamic parameters, natural
undamped frequency, and damping ratio (ref. 4). Frequency-response curves

for various damping ratios are shown in figure 14 in the form of amplitude and phase angles against frequency ratio, defined as the ratio of forced frequency to natural undamped frequency (ref. 5). In order to obtain reliable frequency-response data it is necessary to subject the indicator to sinusoidal pressures of known magnitudes over the frequency range of interest. This range should cover all harmonic components of the pressure fluctuations which the indicator is to measure. In the present instance this would require a sinusoidal pressure source capable of known amplitudes of the order of a few pounds per square inch over the frequency range 0 to 50,000 cycles per second. Such a pressure source is unavailable, all proposed schemes thus far conceived requiring a dependable indicator, heretofore unavailable, for their calibration. Thus direct frequency-response technique does not appear to be suitable for dynamic-calibration purposes.

An alternative method for determining the dynamic performance of such a measuring device is the transient method in which a sudden disturbance, usually a step function, is applied to the instrument. From an experimentally obtained step-function-response curve the natural undamped frequency and damping ratio are readily calculated with the aid of figure 15, in which the damping ratio is found by measurement of the decay of the peaks occurring in the oscillatory response (ref. 5). Frequency-response curves may be obtained by performing a Fourier transformation of the step-function response. More simply, however, when the natural undamped frequency and damping ratio are determined from the step-function response, frequency-response curves are readily obtained by use of figure 14.

The validity of frequency-response curves thus obtained is based on the assumption that the system parameters are constant. If the elastic coefficient, undamped natural frequency, and damping ratio are constant, this is sufficient to satisfy this requirement. Constancy of the elastic coefficient is verified easily by static calibration. Constancy of damping ratio can be shown for an oscillatory transient by choosing different combinations of peak amplitudes. Constancy of natural frequency may be checked directly by time-interval measurements on the transient response record. For the pressure receivers described in this paper these conditions of constancy are well fulfilled, making feasible the use of the transient scheme for a satisfactory dynamic calibration.

To make a transient study of a pressure indicator, a stepwise pressure function of known intensity may be conveniently produced by means of a shock tube (refs. 6 and 7). Figure 16 shows the arrangement of a small shock tube designed for dynamic calibration of high-frequency pressure indicators. It consists of a compression chamber shown at the left and an expansion chamber shown at the right. These two chambers are separated by a cellophane membrane. The thickness of the membrane is selected so it will be just strong enough to withstand the pressure difference between the two chambers. Inside the compression chamber, a sharp-pointed pin is

mounted. This pin extends to the outside of the compression chamber, from where it may be triggered to pierce through the membrane. When this is done, the membrane bursts into hundreds of pieces because of the pressure difference. Immediately after the burst of the membrane the gas from the high-pressure chamber rushes into the expansion chamber and compresses the gas in front of it. A shock-wave front forms as the pressure wave propagates into the low-pressure chamber. When the shock wave reaches the end of the tube, it is reflected according to a well-known law. As the reflected shock wave passes back over the moving gas, it brings the gas to rest at a pressure higher than that following the original shock.

Figure 17 shows the instantaneous pressure distribution inside the shock tube at various time intervals after the burst of the membrane. In the diagram t_0, the initial condition with p_2 in the compression chamber and p_0 in the expansion chamber is shown. At t_1, a shock wave front s with a pressure p_1 is shown propagating toward the expansion chamber. The dotted line c behind the wave front is used to indicate the boundary of the gases that originated from the two chambers. Because the gas to the right of the dotted line c has been compressed from a lower pressure and the gas to the left of this line undergoes an expansion from a higher pressure, a temperature gradient exists across this line.

While the shock wave is propagating toward the expansion chamber a rarefaction wave is propagating toward the compression chamber. Unlike the shock wave, the pressure change in the rarefaction takes place very slowly. The leading edge of this wave is designated by R. Gas is accelerated toward the expansion chamber in the rarefaction wave between R and F and reaches a constant velocity between F and S.

In diagram t_2, a reflected shock wave is formed with a strength of p_3. This reflected shock is shown propagating toward the compression chamber, while the rarefaction wave is reflected from the compression-chamber end wall. In the next three diagrams, the reflected rarefaction wave proceeds toward the right while the reflected shock wave propagates toward the left. During this entire interval the pressure at the surface of the expansion-chamber end wall remains at p_3 until the arrival of the rarefaction wave shown in diagram t_6. Thereafter the pressure would decrease gradually.

In transient study of a pressure indicator, the indicator may be conveniently installed on the expansion-chamber end wall. Figure 18 shows the pressure variation at the expansion-chamber end wall plotted as a function of time. The important point of the plot is the existence of a sharp step function at the moment of the arrival of the shock wave.

At this moment pressure changes from the expansion-chamber pressure p_o to the reflected-wave pressure p_3 without realizing the original-shock-wave pressure p_1. Another important point is the constant-pressure interval after the initial step function.

The usefulness of a shock tube as a step-function generator for transient study of a pressure indicator depends upon the realization of the following characteristics:

(a) A pressure rise time much shorter than the natural period of the indicator

(b) A constant-pressure duration longer than 10 times the natural period of the indicator

(c) A known amount of pressure change

(d) A minimum amount of interference

Rise Time of Shock-Wave Function

The pressure rise time across a shock front is equal to the thickness of the shock wave divided by its speed. According to kinetic theory of gas, the thickness of the wave front is equal to a few mean free paths of the gas molecules. In room temperature this thickness is of the order of 0.0001 inch. Assume that the shock speed is of the neighborhood of room temperature sound speed of air. Then the pressure-rise time of a normal shock is less than 10^{-8} second, which is much shorter than the natural period of any indicator. In the case of a reflected shock, the pressure-rise time is affected by the imperfection of the surface at the end wall. Assuming that the imperfection has a depth of $1/100$ inch, then the pressure rise time is 10^{-6} second, which is still considerably shorter than the natural period of the indicator.

Duration of Reflected Shock

The duration of the constant high pressure of the reflected shock may be computed from the speed of the shock wave, the speed of the rarefaction waves, and the chamber lengths according to a fairly involved relationship. In the calibration of the indicators it is found, however, that a simple empirical formula as shown below is sufficient.

$$t_{p_3} = \frac{2L}{a_o} \tag{7}$$

where

t_{p_3} time interval of reflected shock at pressure p_3

L   length of compression chamber

a_0 undisturbed sound speed of gas

For instance, when helium is used with a 2-foot compression chamber, the high-pressure duration is approximately 0.0012 second. Use the same compression chamber with air as the medium and it would yield a high-pressure duration of approximately 0.0035 second. Both these figures are sufficient for testing indicators with a natural frequency above 10,000 cycles per second.

Magnitude of Reflected Shock Wave

Von Neumann (ref. 8) has shown that the pressure of the reflected shock p_3 may be computed from the pressure ratio ξ of the normal shock:

$$\xi' = \frac{p_1}{p_3} = \frac{1 + \eta\xi}{\eta + 2 - \xi} \tag{8}$$

where

$$\xi = \frac{p_0}{p_1}$$

$$\eta = \frac{\gamma + 1}{\gamma - 1}$$

$$\gamma = \frac{c_p}{c_v}$$

For air $\gamma = 1.4$ and $\eta = 6$ and for helium $\gamma = 1.63$ and $\eta = 4.15$.

The value of ξ may be obtained from the initial pressure ratio p_0/p_2 of the two chambers.

$$\frac{p_o}{p_2} = \xi \left[1 - \frac{a_{oe}}{a_{oc}} \frac{\eta_e - 1}{\eta_c - 1} \frac{1 - \xi}{\sqrt{(\eta_e + 1)\xi(\eta_e + \xi)}} \right]^{\eta_c + 1} \tag{9}$$

where a_o is the undisturbed sound speed and subscripts c and e indicate parameters pertaining to compression chamber and expansion chamber, respectively. When the same gas is used in each chamber, equation (9) reduces to

$$\frac{p_o}{p_2} = \xi \left[1 - \frac{1 - \xi}{\sqrt{(\eta_e + 1)\xi(\eta_e + \xi)}} \right]^{\eta + 1} \tag{10}$$

For air where $\eta = 6$

$$\frac{p_o}{p_2} = \xi \left[1 - \frac{1 - \xi}{\sqrt{7\xi(6 + \xi)}} \right]^{7} \tag{11}$$

and for helium where $\eta = 4.15$

$$\frac{p_o}{p_2} = \xi \left[1 - \frac{1 - \xi}{\sqrt{5.15\xi(4.15 + \xi)}} \right]^{5.15} \tag{12}$$

Equations (8), (11), and (12) are useful to find the relation between the known pressure difference of the two chambers and the step function applied to the indicator. The results of using these equations are shown in figure 19.

Interference in Shock Wave

In an ideal case, a pure step function is required to calibrate the indicator. This necessitates the generation of a true plane shock wave and a true plane reflected wave. Any deviation from these conditions produces interferences. In practice, a true plane wave cannot be formed immediately after the shattering of the membrane because the membrane does not just disappear in an infinitesimal period of time. However, as the shock is propagating toward the expansion chamber it has the tendency to form a stable plane wave. This requires time and therefore a longer expansion chamber provides a cleaner shock. In experimenting with indicators in a 2-inch shock tube it has been found that the minimum length of the expansion chamber is about 4 feet when helium is used and 6 feet when air is used.

As for the generation of a plane reflection wave, the controlling factor is the perfection of the expansion-chamber end wall. To get a good result the wall should be perpendicular to the center line of the tube within 1 or 2 thousandths of an inch. The corner between the end wall and the side wall should be square and without appreciable open seam. The surface of the end wall and the adjacent side wall should be made with reasonably good finish. Above all, when the indicator is assembled in the end wall the pressure receiver should be flush with the inner surface of the end wall. A cavity or a protrusion formed by the pickup is highly objectionable. To obtain the best result it is advisable to fill the seam around the end of the threaded portion of the pickup with sealing wax.

For indicators which are relatively sensitive to vibration effect another type of interference called the "ground shock" may be noticed. Ground shock is the shock wave that is transmitted through the side wall of the expansion chamber. This type of interference usually precedes the gas shock wave because sound speed of the chamber wall is faster than the sound speed of gas. If ground shock becomes objectionable it may be eliminated by mounting the pickup on a rubber end wall.

TEST RESULTS

The transient response record of a pressure indicator may be obtained with a cathode-ray oscilloscope and a high-film-speed camera. In general, a drum-type camera would be most satisfactory for this purpose. However, because of its availability, a strip film camera with a film speed of 400 inches per second was used in the test.

Two methods were used to coordinate the signal with time reference. In the first method the pressure signal axis was arranged perpendicular to the film travel axis. The result is recorded with time as the horizontal axis. In the second method the film was driven in the same direction as the axis of the pressure signal while a horizontal saw-tooth sweep function was applied. In this method the pressure-time diagram is distorted and cut into sections, but at the same time is expanded to allow accurate count of the oscillations.

Figure 20 shows the transient response of a high-pressure strain-gage indicator obtained by the first recording method. In this diagram the envelope of the oscillation is clearly shown. Figure 21 shows the transient response of the same indicator obtained by the second recording method with 2,000-cycle-per-second sweep frequency. There are 24 oscillations to each sweep which yields a natural frequency of 48,000 cycles per second. The damping ratio of the instrument can be estimated from the exponential envelope of the oscillations shown in both figures. For this indicator the damping ratio is about 0.035.

Figure 22 gives the transient response of a low-pressure-type strain-gage indicator. This figure shows a natural frequency of 21,000 cycles per second plus a beat frequency. The cause of this beat effect is not exactly known.

Figure 23 shows the transient response of a 5/16-inch spherical-diaphragm indicator.

Figure 24 shows the expanded record of the same indicator. The natural frequency of this indicator is about 60,000 cycles per second. The relatively slow rise in pressure signal may be partially due to the curvature of the diaphragm and partially due to the electronic system.

Figure 25 shows the transient response of the electronic system of this indicator.[1] In this figure a time delay is also shown and the response curve is quite similar to that of figure 24. This indicates the performance of the spherical diaphragm is approaching that of the electronic circuit. A better circuit is required to explore fully the performance of this pickup.

Figure 26 shows the transient response of a 1/2-inch flat-diaphragm indicator with a sensitivity of the same order of the 5/16-inch spherical-diaphragm indicator. In this figure the natural frequency of the flat diaphragm is shown as around 12,000 cycles per second or one-fifth that of the spherical diaphragm. The transient is many times larger than that shown in figure 24 and so is the ground shock. A comparison between figures 24 and 26 clearly demonstrates the advantage of using a spherical diaphragm instead of a flat diaphragm.

CONCLUDING REMARKS

The effective mass per unit area and the interference level of a pressure receiver determine the over-all performance of a pressure indicator. To reduce the mass, it is necessary to use an efficient structural design. A dome-shaped or spherical diaphragm is shown to be superior to a flat diaphragm in this respect. The interferences of a pressure indicator may be classified into several categories. The dome-shaped diaphragm is the best from the standpoint of vibration interference. Catenary diaphragms have very small temperature interferences and are also reasonably insensitive to vibration.

[1] In testing transient response of the electronic system, an additional capacitor is arranged in a circuit parallel with the capacitance of the indicator. The size of this capacitance is equivalent to the change of capacitance of the indicator under test pressure. The lead wire of this parallel capacitor may be sheared off to produce the desirable transient test.

Of the mechanical-electrical transducers, the wire strain gage leads in simplicity. The capacitance type is more versatile because it permits the use of very high frequency carrier systems and thereby cuts down the effective interference in the electronic system. Barium titanate produces large signals without excitation and results in compact design. Barium titanate can only be used for dynamic measurement when temperature variations are slight.

Since no instrument has an all-round performance, it is sometimes necessary to use several methods to make one type of pressure measurement.

Massachusetts Institute of Technology,
    Cambridge, Mass., October 10, 1952.
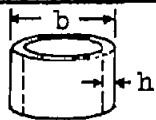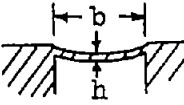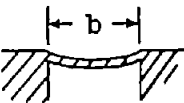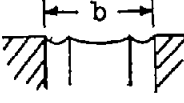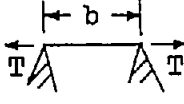
REFERENCES

1. Draper, C. S., and Li, Y. T.: A New High-Performance Engine Indicator
   of the Strain-Gage Type. Jour. Aero. Sci., vol. 16, no. 10, .Oct.
   1949, pp. 593-610.

2. Grinstead, C. E., Frawley, R. N., Chapman, F. W., and Schultz, H. F.:
   An Improved Indicator for Measuring Static and Dynamic Pressures.
   S.A.E. Jour., vol. 52, no. 11, Nov. 1944, pp. 534-556.

3. Greenwood, Ivan A., Holdam, J. Vance, and MacRae, Duncan, eds.:
   Electronic Instruments. First ed., McGraw-Hill Book Co., Inc.,
   1948.

4. Taback, Israel: The Response of Pressure Measuring Systems to Oscil-
   lating Pressures. NACA TN 1819, 1949.

5. Draper, Charles Stark, McKay, Walter, and Lees, Sidney: Instrument
   Engineering. First ed., McGraw-Hill Book Co., Inc., 1952.

6. Geiger, Fred W., and Mautz, C. W.: The Shocktube as an Instrument
   for the Investigation of Transonic and Supersonic Flow Patterns.
   Project No. M 720-4, Contract N6-ONR-232, Office of Naval Res.,
   and Eng. Res. Inst., Univ. Mich., 1949.

7. Perls, Thomas A.: A New Condenser-Type Pressure Gage. Rep. No. 625,
   TED TMB 2406, The David W. Taylor Model Basin, Bur. Aero., Navy Dept.,
   June 1949.

8. Von Neumann, John: Progress Report of Theory of Shock Waves. Rep.
   No. 1140, OSRD and Princeton Univ., Jan. 29, 1943.

9. Den Hartog, Jacob Pieter: Mechanical Vibrations. Third ed., McGraw-
   Hill Book Co., Inc., 1947.

10. Timoshenko, S.: Theory of Plates and Shells. McGraw-Hill Book Co.,
    Inc., 1940.

11. Rayleigh, (Lord) John William Strutt: The Theory of Sound. Second
    ed., Macmillian & Co., Ltd. (London), 1929.

12. Patterson, John L.: A Miniature Electrical Pressure Gage Utilizing a
    Stretched Flat Diaphragm. NACA TN 2659, 1952.

TABLE I.- PRESSURE-RECEIVER CHARACTERISTICS

[Data obtained from refs. 9 to 12. ω_n, natural frequency; λ, speed of sound in receiver material; m_e, effective mass of receiver; m, total mass of receiver; E, modulus of elasticity; h, thickness of receiver; y, depth of spherical diaphragm; ϵ, tension per unit length; σ_{max}, maximum allowable stress; l, length of strain tube; p_{max}, maximum allowable pressure]

Pressure-receiver type	Schematic diagram	$\dfrac{\omega_n}{\lambda} b$	$S \dfrac{E}{b}$	m_e/m	p_{max}/σ_{max}	Remarks
Cylinder		2	$0.25 \dfrac{b}{h}$	1	$2 \dfrac{h}{b}$	Poor acoustic coupling
Flat diaphragm		$12.2 \dfrac{h}{b}$	$0.011 \dfrac{b^3}{h^3}$	0.6	$\dfrac{4}{3} \dfrac{h^2}{b^2}$	Most simple in construction
Spherical diaphragm		[a]$16 \dfrac{y}{b}$	$0.0058 \dfrac{b}{h} \dfrac{b^2}{y^2}$	$1/6$	$16 \dfrac{y}{b} \dfrac{h}{b}$	Best high-frequency acoustic
Catenary diaphragm		[b]$1.76 \dfrac{b}{l}$	$0.202 \dfrac{l}{h}$	1.60	$2.82 \dfrac{h}{b}$	Best temperature compensation
Membrane		$4.8 \sqrt{\dfrac{\epsilon}{E}}$	$0.13 \dfrac{E}{\epsilon} \dfrac{b}{h}$	0.7	$8.8 \dfrac{h}{b} \sqrt{\dfrac{\sigma_{max} - \epsilon}{E}}$	Limited to low-frequency application only

[a]$y/b < 1/10.$

[b]$l \approx b.$

TABLE II.- PERFORMANCE CHARACTERISTICS OF A SPHERICAL-DIAPHRAGM

INDICATOR WITH CAPACITIVE TRANSDUCER

Maximum pressure, lb/sq in.	50
Minimum detectable pressure, in. H_2O	1
Natural frequency (from shock tube)	
cps	60,000
Diaphragm diameter, in.	5/16
Depth ratio	1/30
Zero shift, lb/sq in./^{O}F	1/10
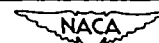
TABLE III.- PERFORMANCE CHARACTERISTICS OF LOW-PRESSURE

STRAIN-GAGE-TYPE PRESSURE INDICATORS

Diaphragm diameter, in.	5/16	5/16	1/2
Diaphragm thickness, in.	0.001	0.003	0.002
Back pressure, lb/sq in. gage	40	0	40
Maximum pressure, lb/sq in. gage	30	30	30
Natural frequency, cps	20,000	15,000	15,000
Minimum detectable pressure, in. H_2O	1	0.5	0.5
Zero shift with temperature, lb/sq in./^{O}F . . .	0.005	0.02	0.005

TABLE IV.- PERFORMANCE OF BUTTON-SIZED BARIUM-TITANATE

PRESSURE INDICATOR

Diaphragm diameter, in.	1/2
Rated pressure, lb/sq in.	50
Natural frequency, cps	15,000
Minimum detectable pressure, in. H_2O	0.02
Zero shift, lb/sq in./°F	1/10
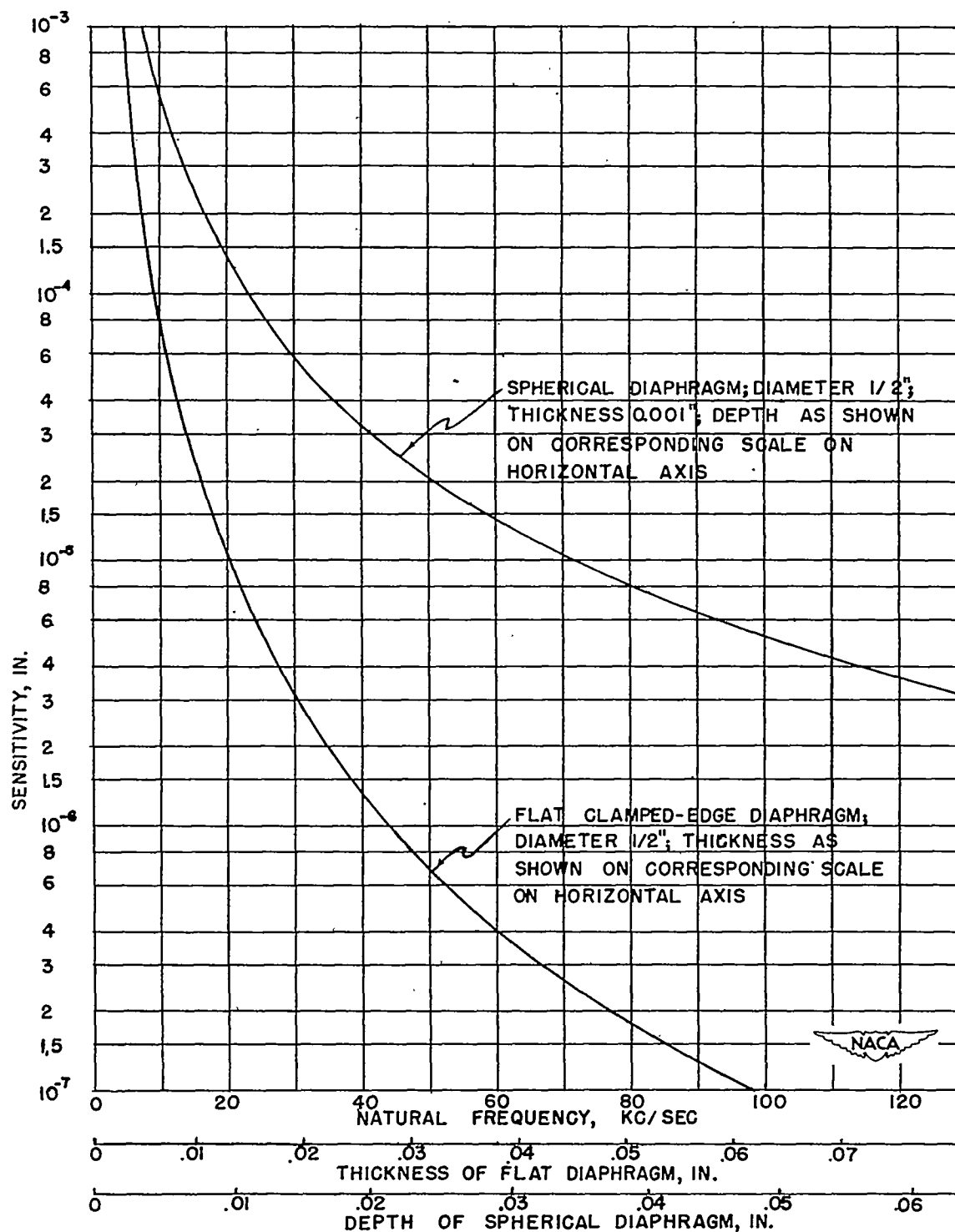
Figure 1.- Performance of spherical diaphragm as compared with that of flat diaphragm.

RADIUS OF
CURVATURE = $\frac{3''}{4}$

OUTPUT
CONNECTOR

TRANSFORMER COILS

DOME - SHAPED DIAPHRAGM
AND ELECTRODE
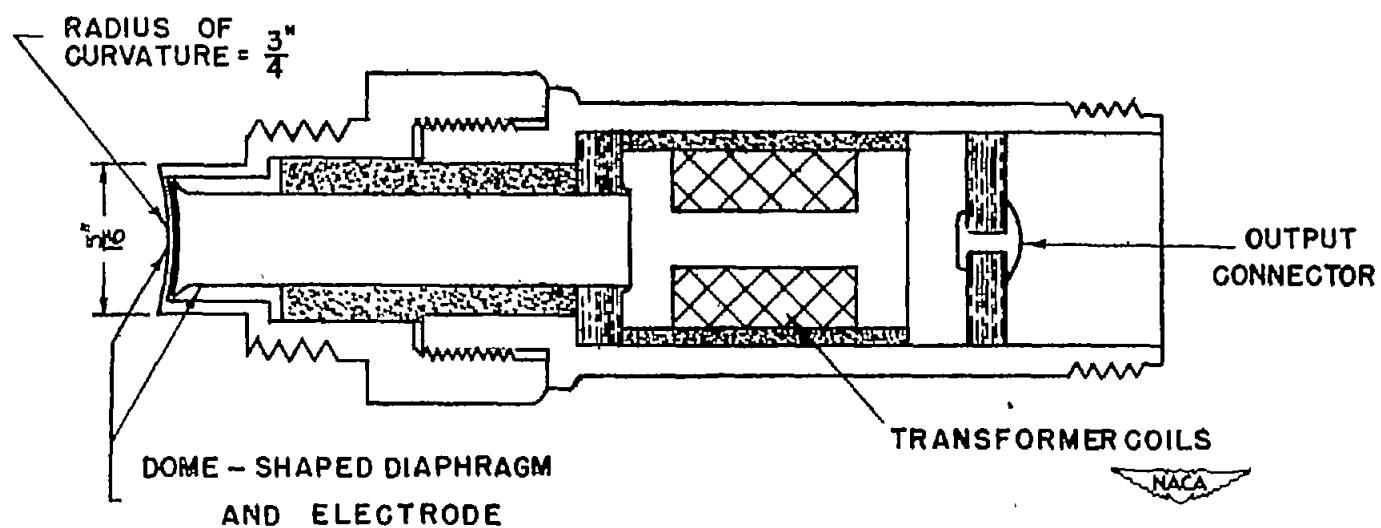
Figure 2.- Semischematic section view of a spherical diaphragm variable-
capacitance-type pressure indicator.
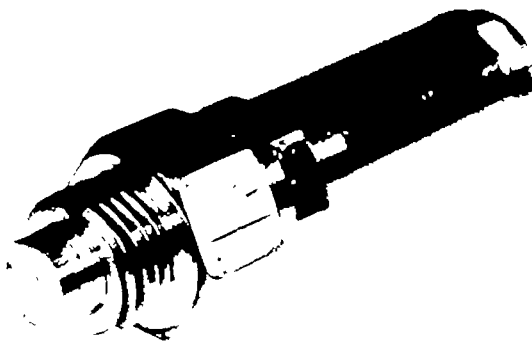
L-80241

Figure 3.- Photograph showing 5/16-inch spherical-diaphragm pressure
   indicator with pressure range of 0 to 30 pounds per square inch
   and a normal frequency of 67,000 cycles per second.
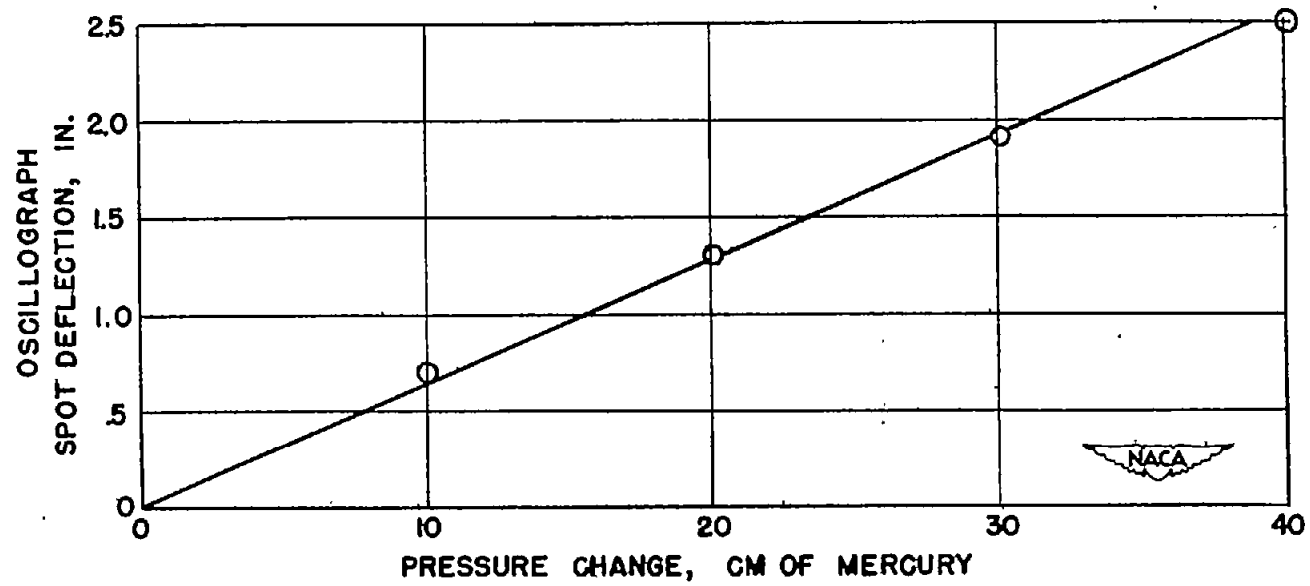
Figure 4.- Static calibration of 5/16-inch spherical-diaphragm variable-capacitance indicator.

CONNECTOR

CONNECTOR
SLEEVE

WIRE CONNECTION

STRAIN-GENERATING-
TUBE SUPPORT
FLANGE

COOLING INSERT

COOLING-AIR GUIDE
TUBE FLANGE

COOLING - AIR
GUIDE   TUBE

LOCATING SHOULDER

STRAIN-GENERATING
TUBE

COOLING-AIR
EXIT   HOLE

FORCE FIT AND
SILVER-SOLDER
JOINT

SHELL

COOLING-AIR
PASSAGE HOLE

NACA

CATENARY DIAPHRAGM
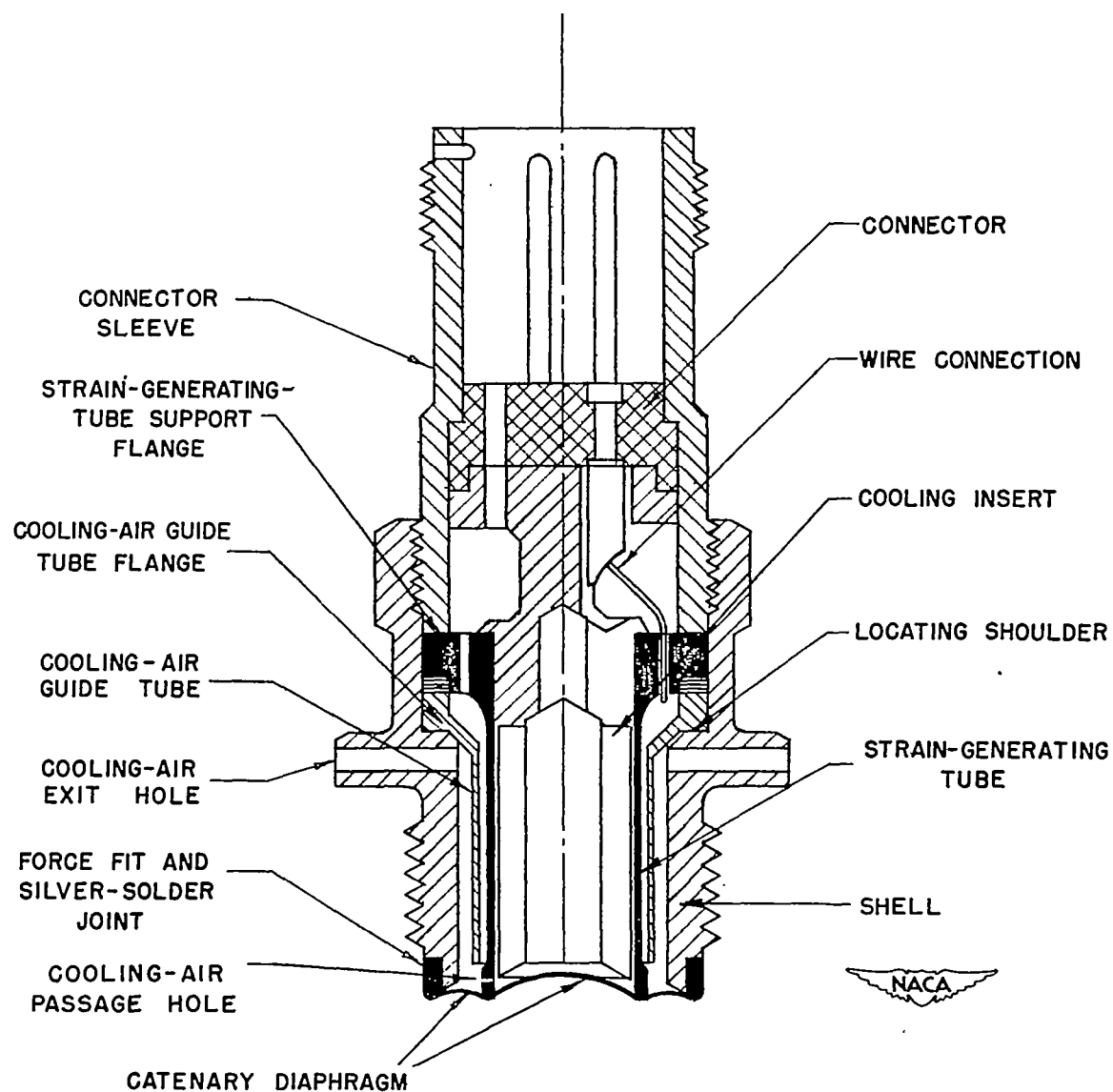
Figure 5.- Cross section of strain-gage indicator with catenary diaphragm.
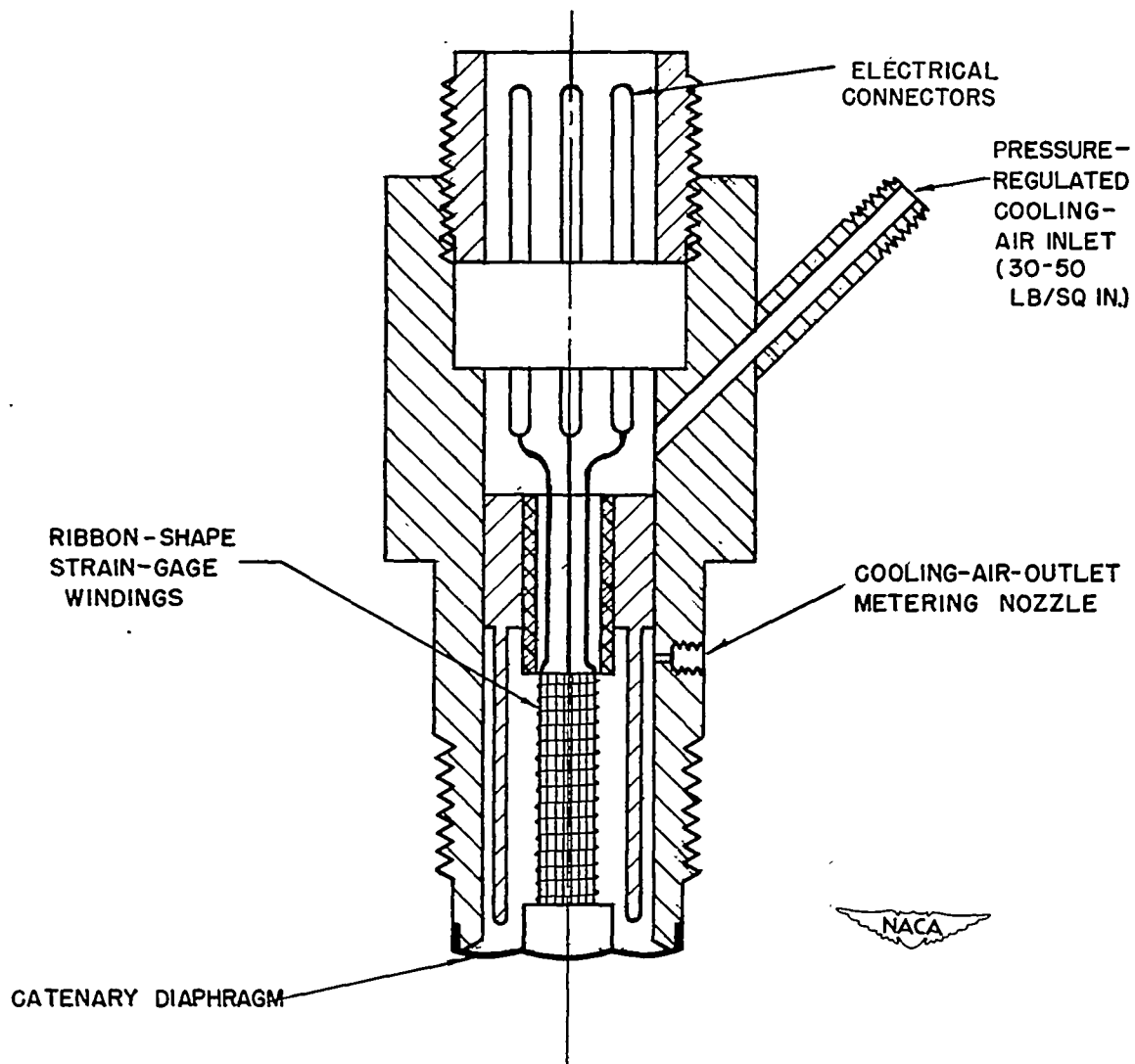
Figure 6.- Low-pressure high-frequency strain-gage pressure indicator.
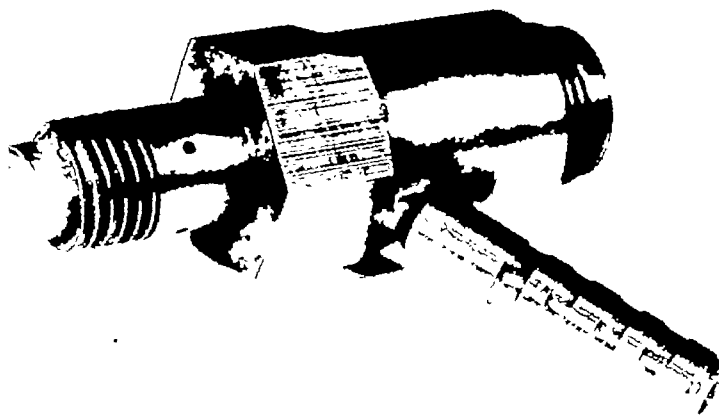
Figure 7.- Photograph showing 5/16-inch strain-gage pressure indicator with pressure range of 0 to 30 pounds per square inch and a normal frequency of 20,000 cycles per second.   L-80242
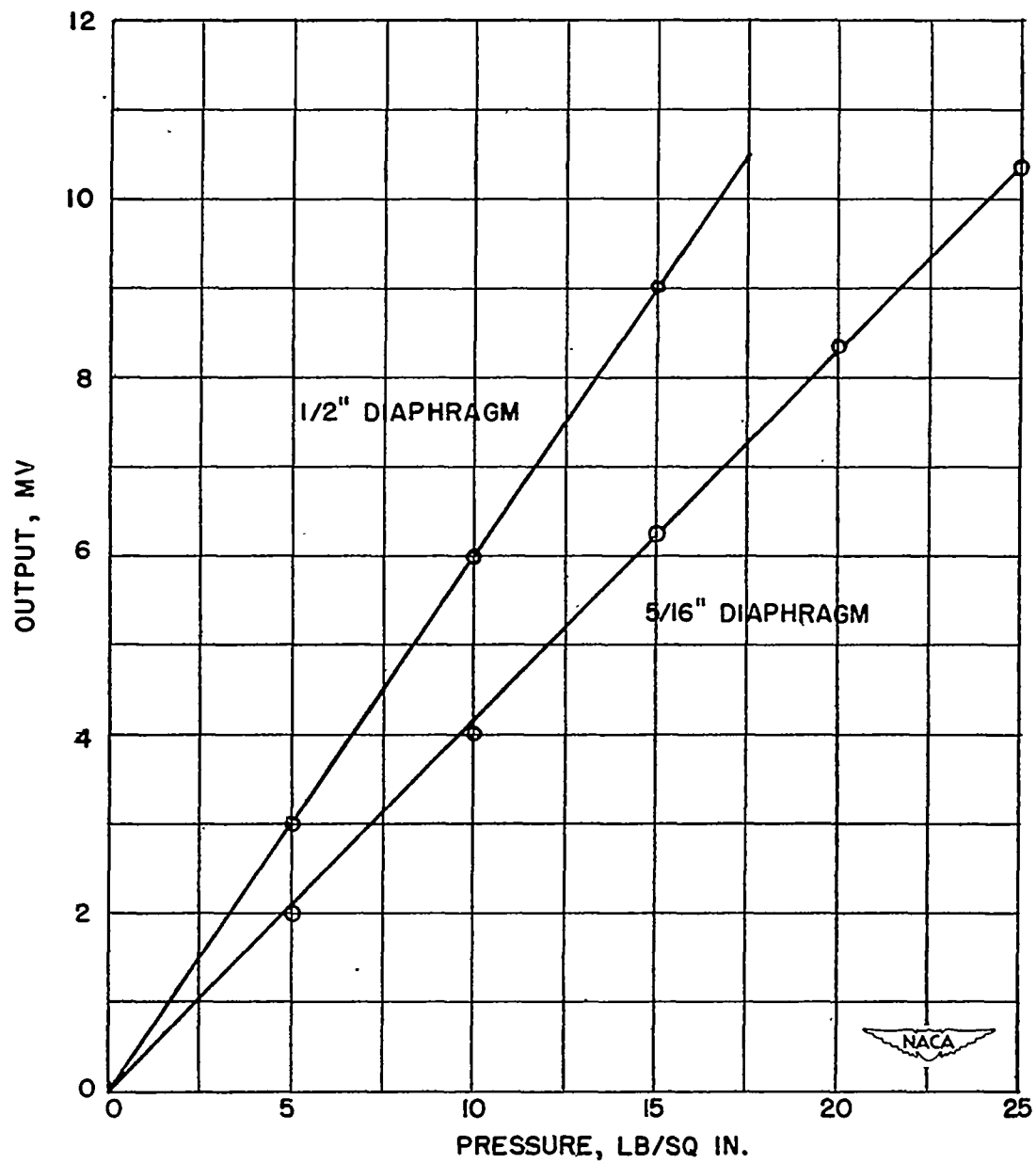
Figure 8.- Static calibration of strain-gage—catenary-diaphragm indicator
of low-pressure type. Excitation is 6 volts.
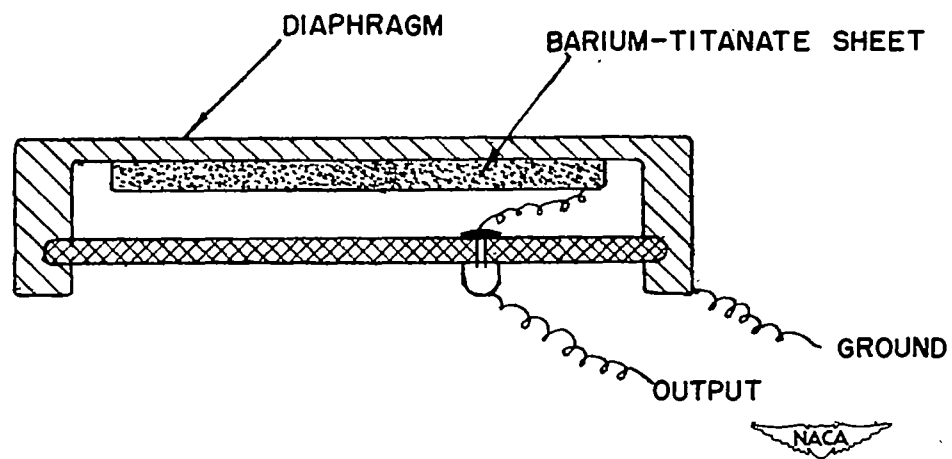
Figure 9.- Construction of barium-titanate pressure pickup.
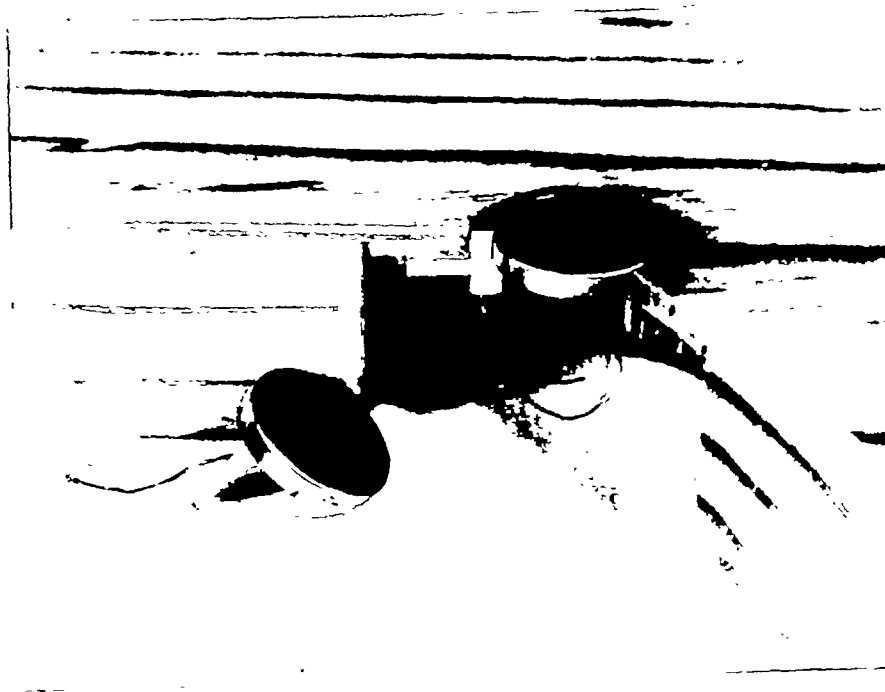
L-80243

Figure 10.- Photograph showing 1/2-inch barium-titanate pressure pickup
and its installation in a model wing.
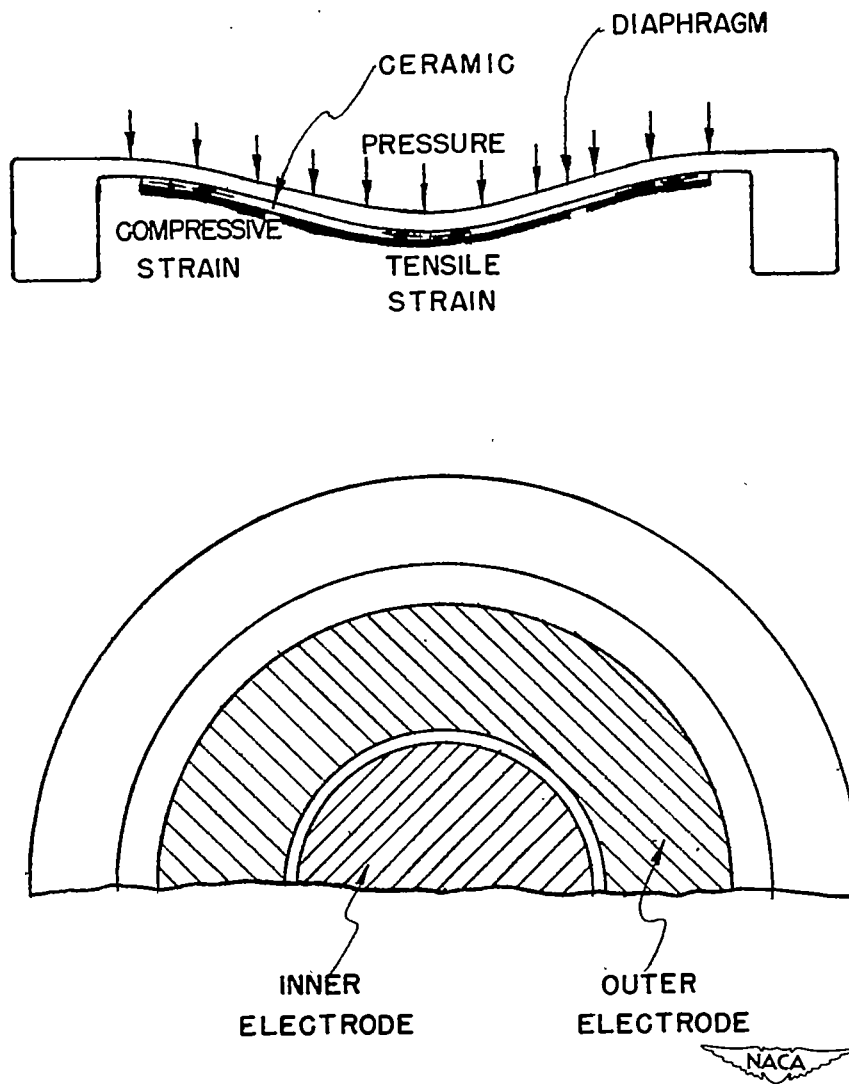
Figure 11.- Temperature compensation scheme of barium-titanate pressure
pickup.
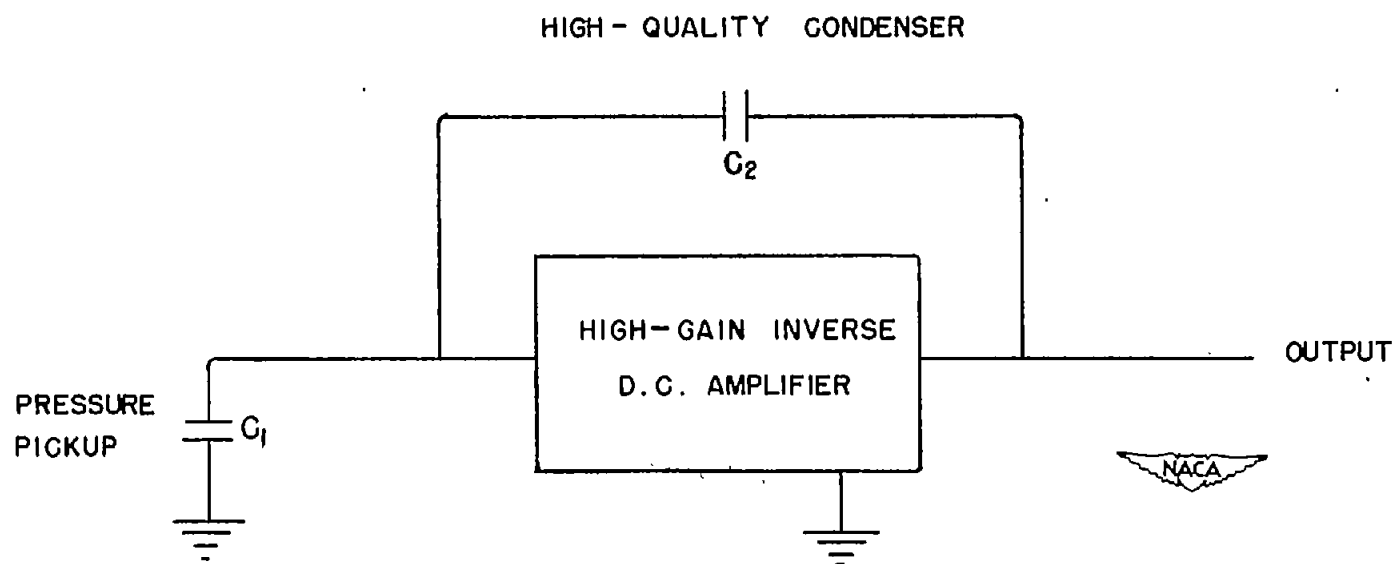
Figure 12.- Schematic diagram of an electrical circuit to improve low-frequency response of barium-titanate pressure pickup.
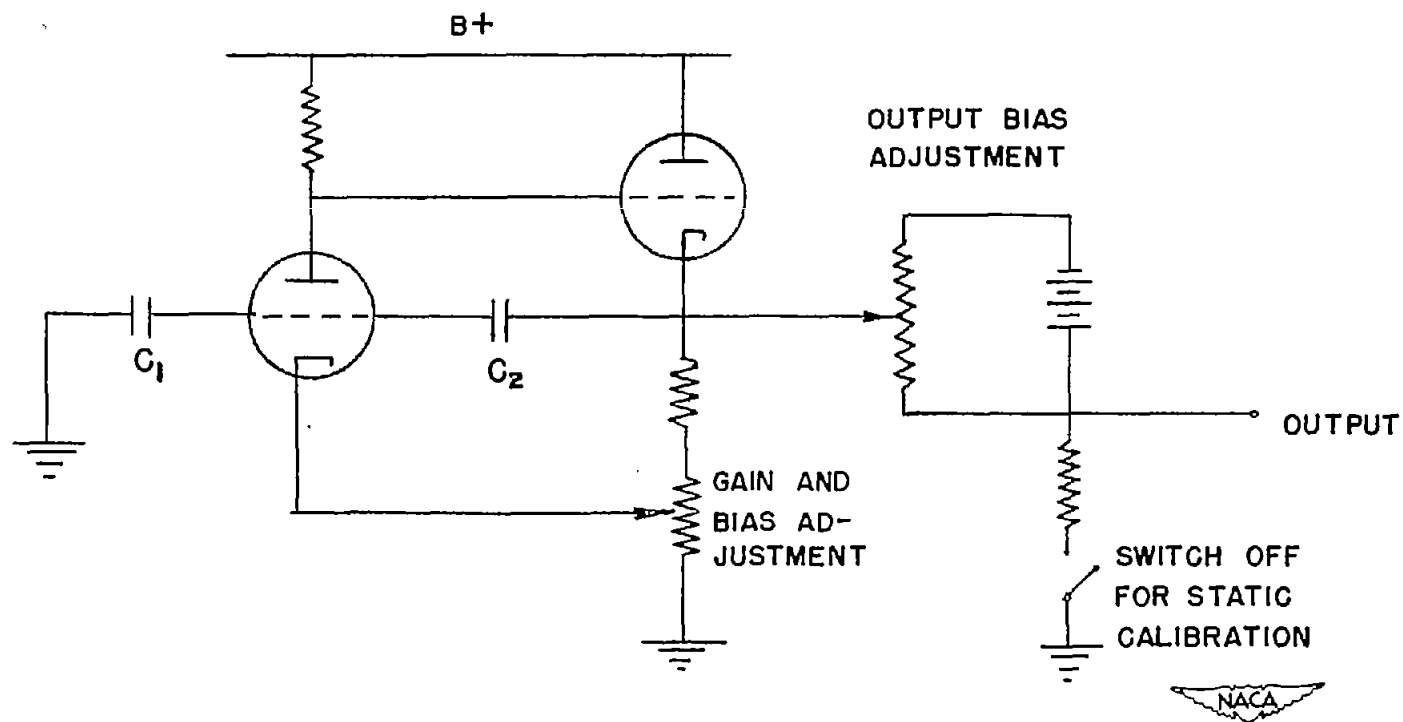
Figure 13.- Basic circuit used for improving low-frequency response of barium-titanate pressure pickup.
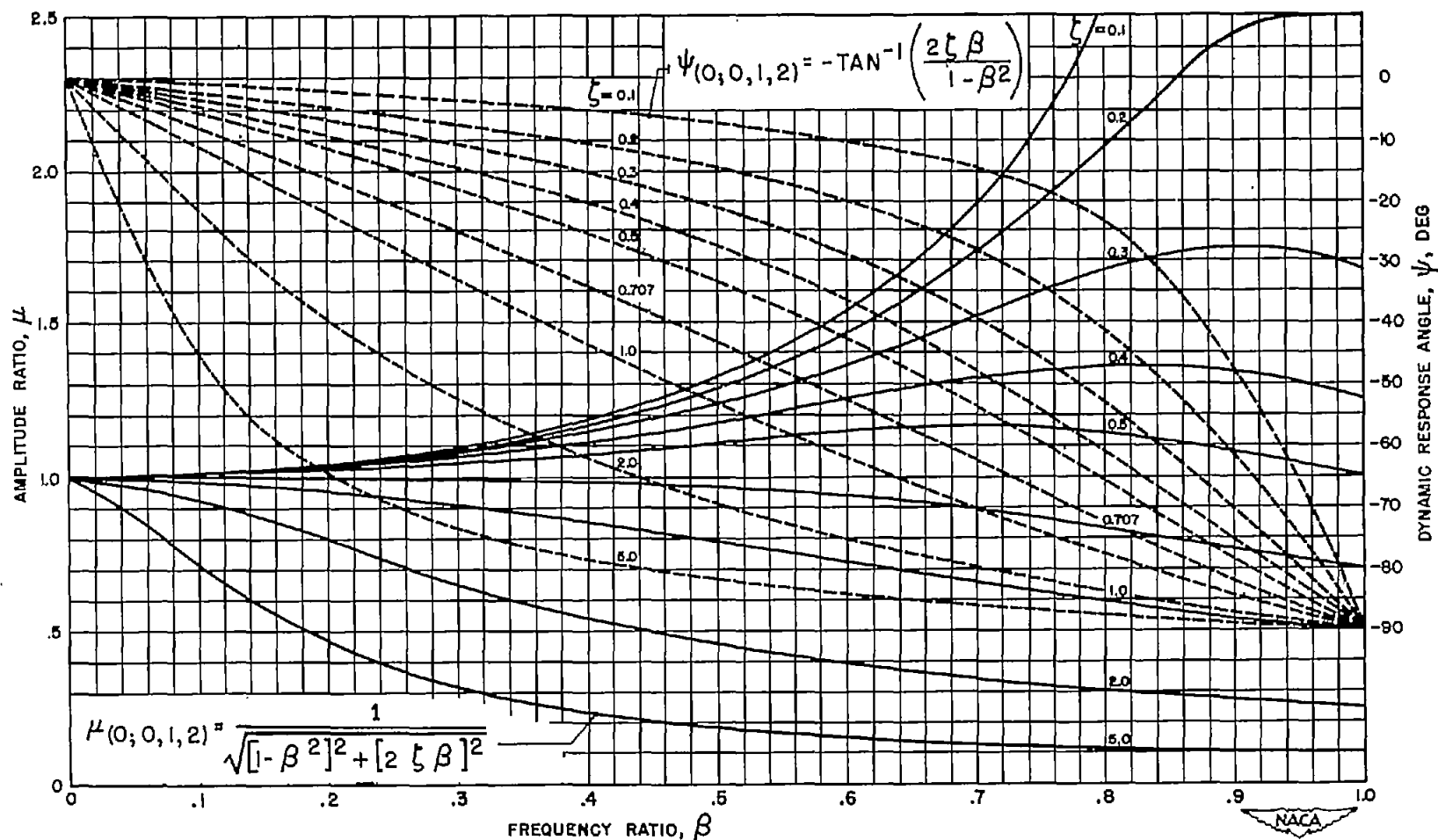
Figure 14.- Steady-state sinusoidal response characteristics associated with differential

equation $\dfrac{1}{\omega_n^2}\ddot{v} + \dfrac{2\zeta}{\omega_n}\dot{v} + v = su$ where u is the independent variable and v is the

dependent variable.
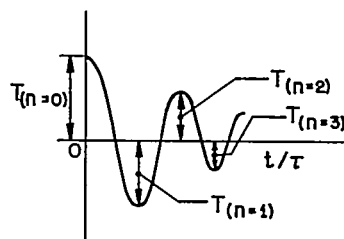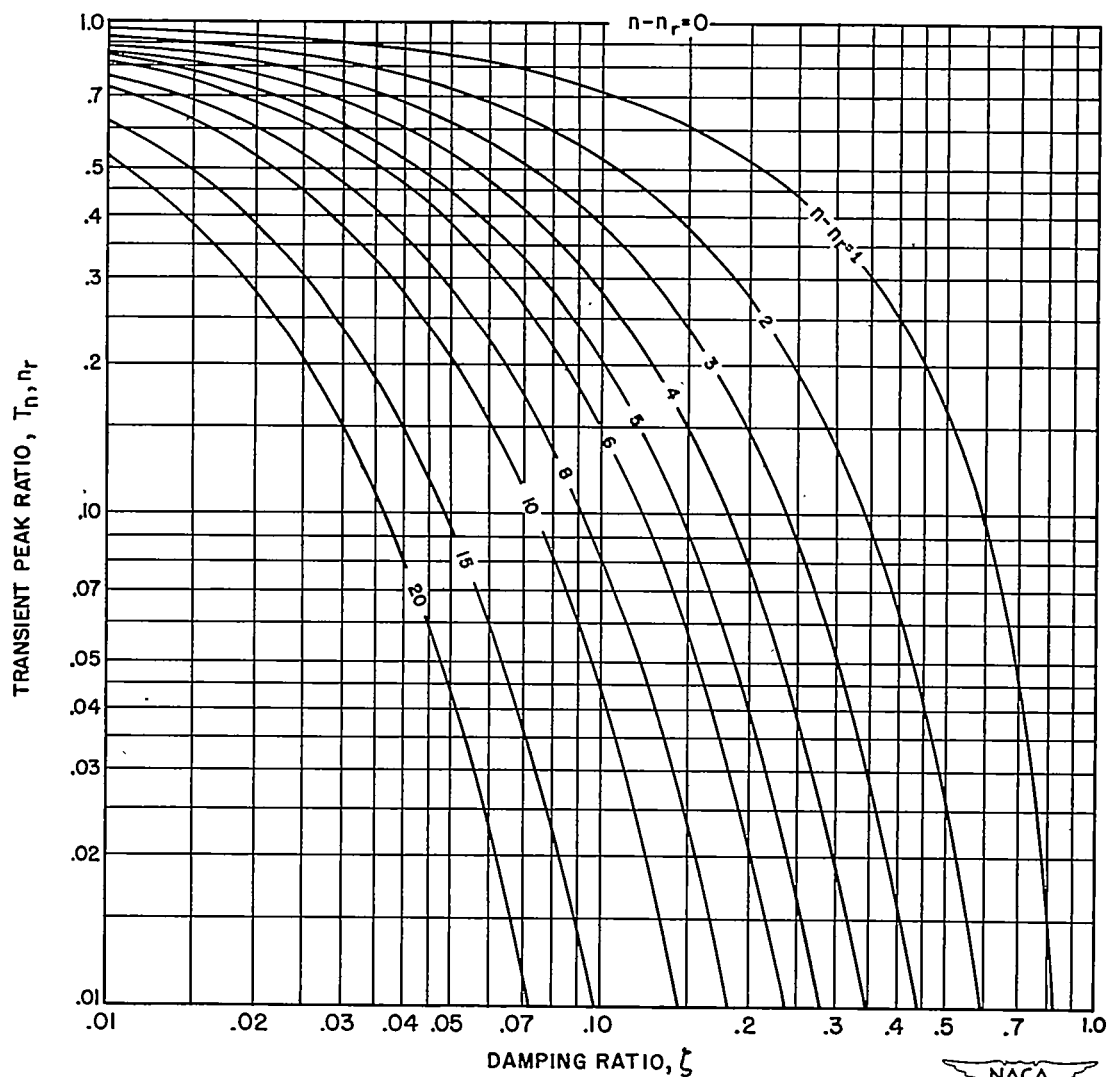
Figure 15.- Logarithmic plot of relationship of transient peak ratio $T_{n_r,n}$ to damping ratio ζ for various values of $n - n_r$ for transient solution of second-order differential equation with constant coefficients when solution is oscillatory. n and n_r are order integers of transient peaks; n_r can be chosen at any peak.
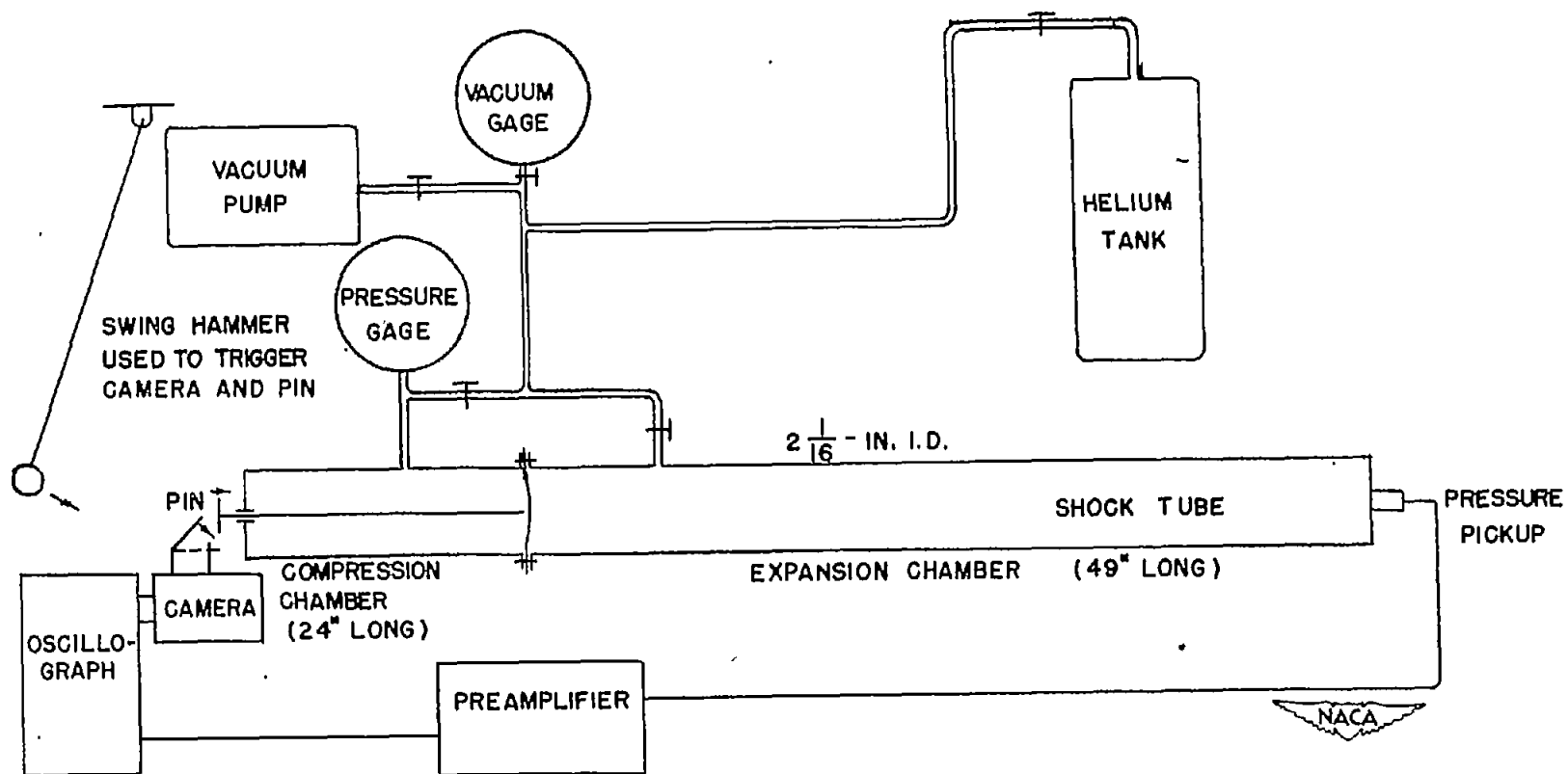
Figure 16.- Schematic diagram of simple shock tube and recording system used in transient study of indicator performance.
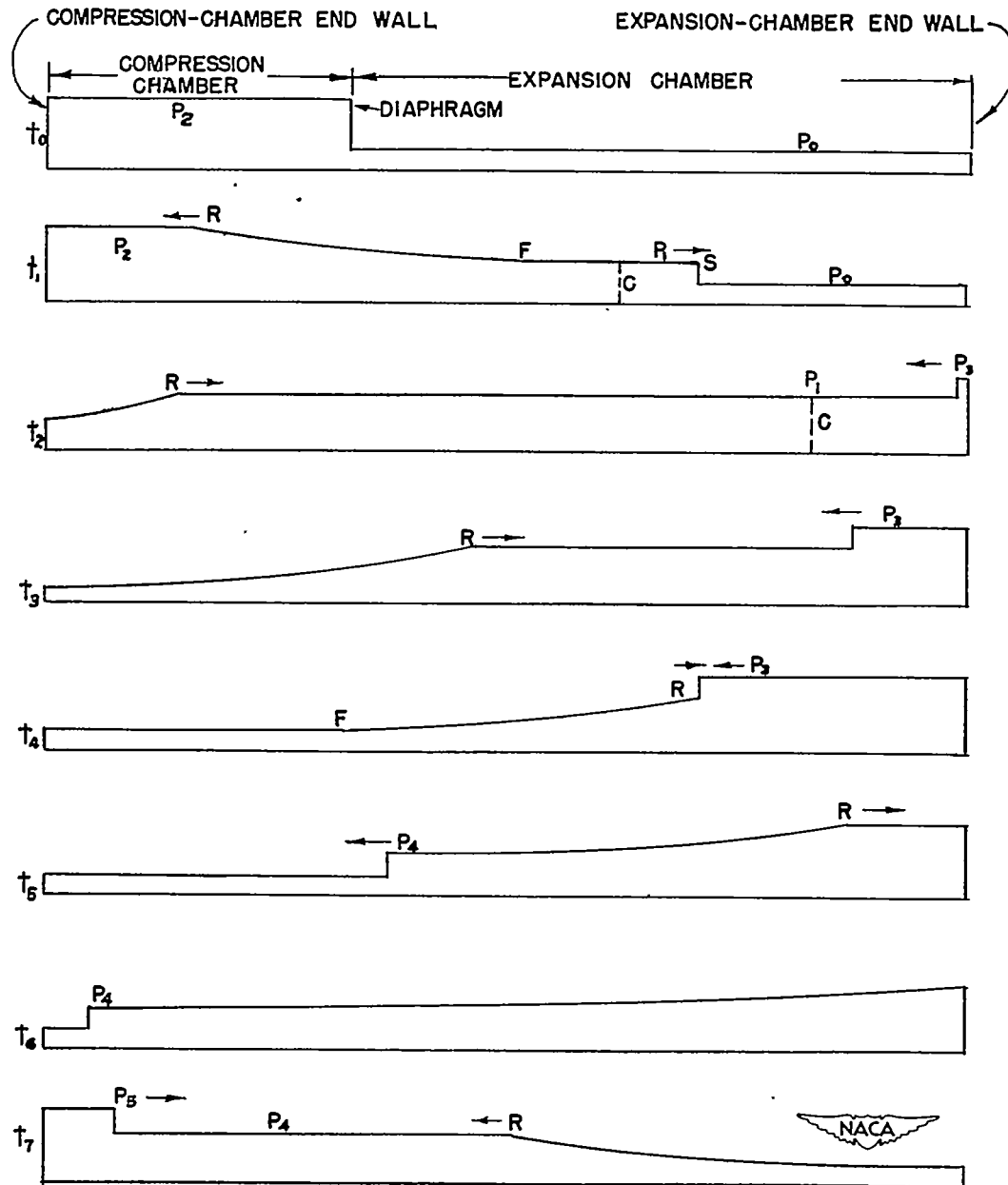
Figure 17.- Pressure distribution in a shock tube at intervals after burst of diaphragm.
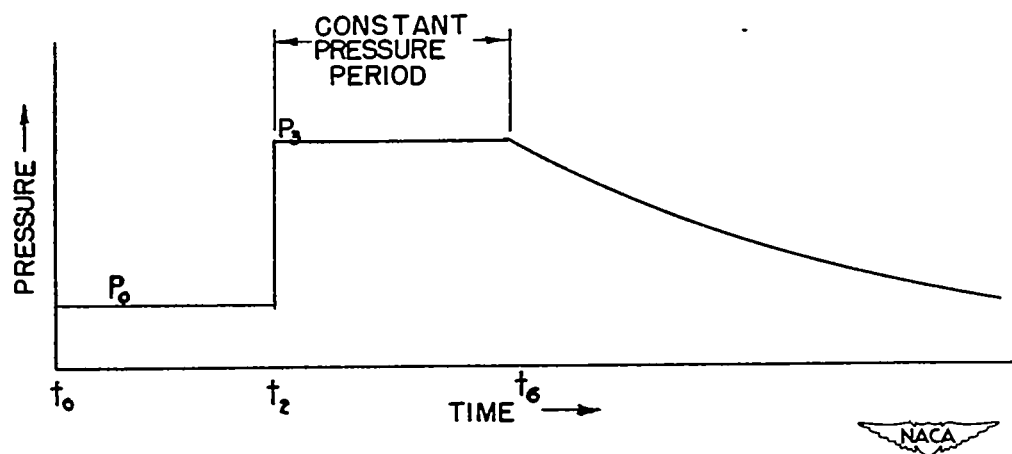
Figure 18.- Pressure-time diagram at surface of expansion-chamber end wall.
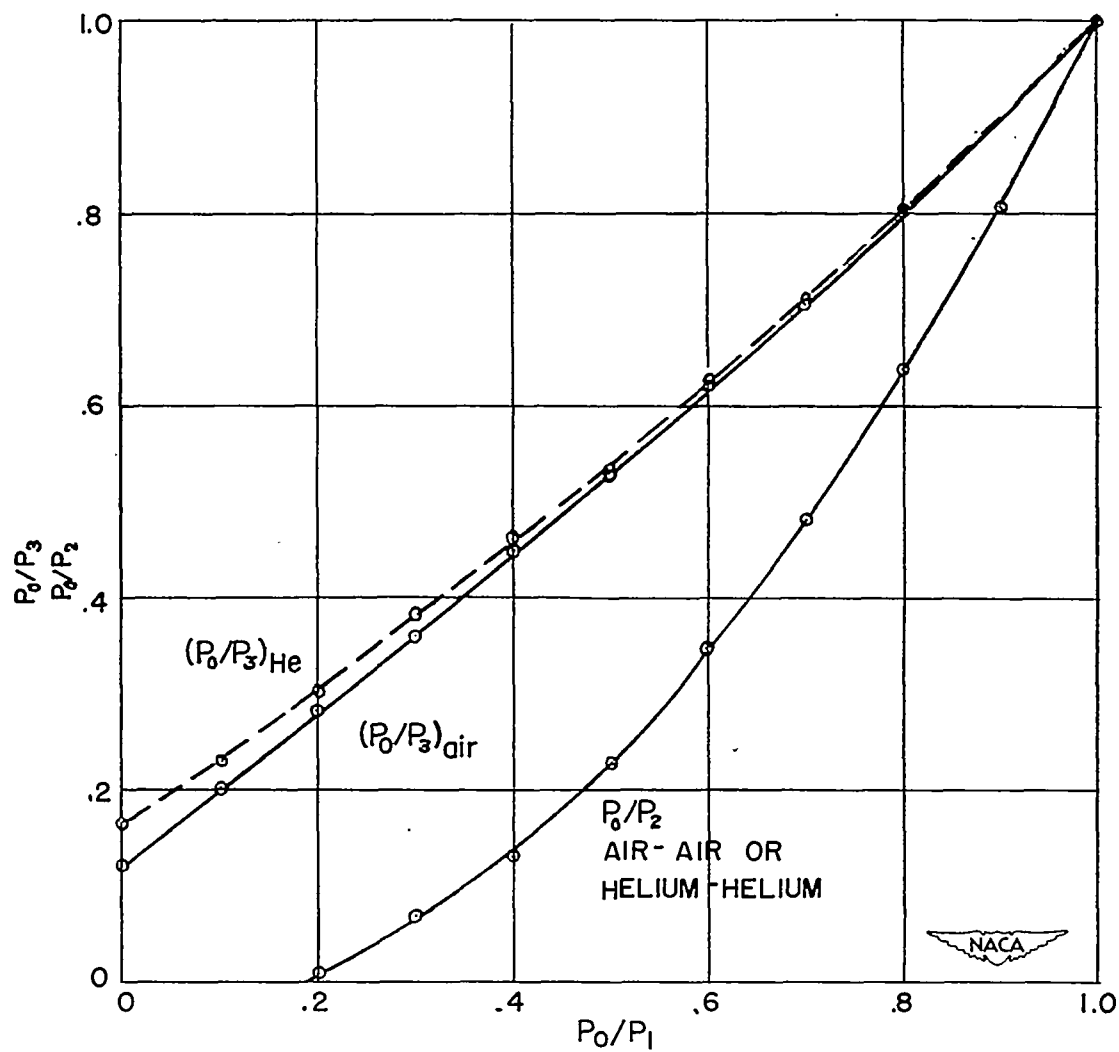
Figure 19.- Shock wave and reflected shock strength with air or helium as medium.
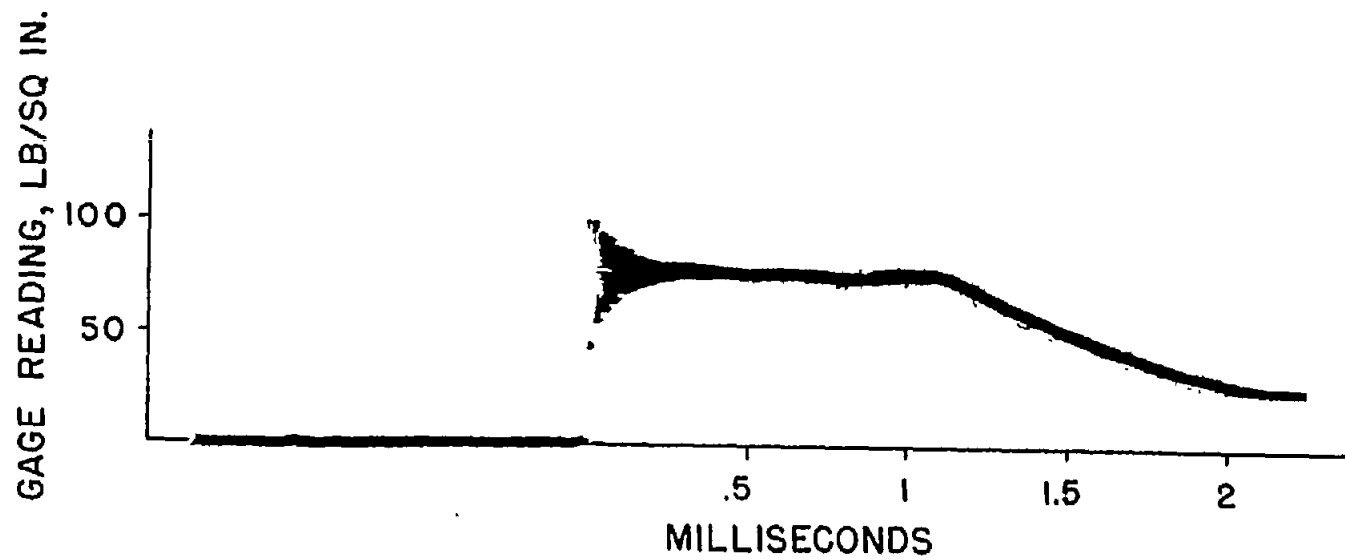
Figure 20.- Transient response of 18-millimeter 1,000-pound-per-square-inch strain-gage indicator.
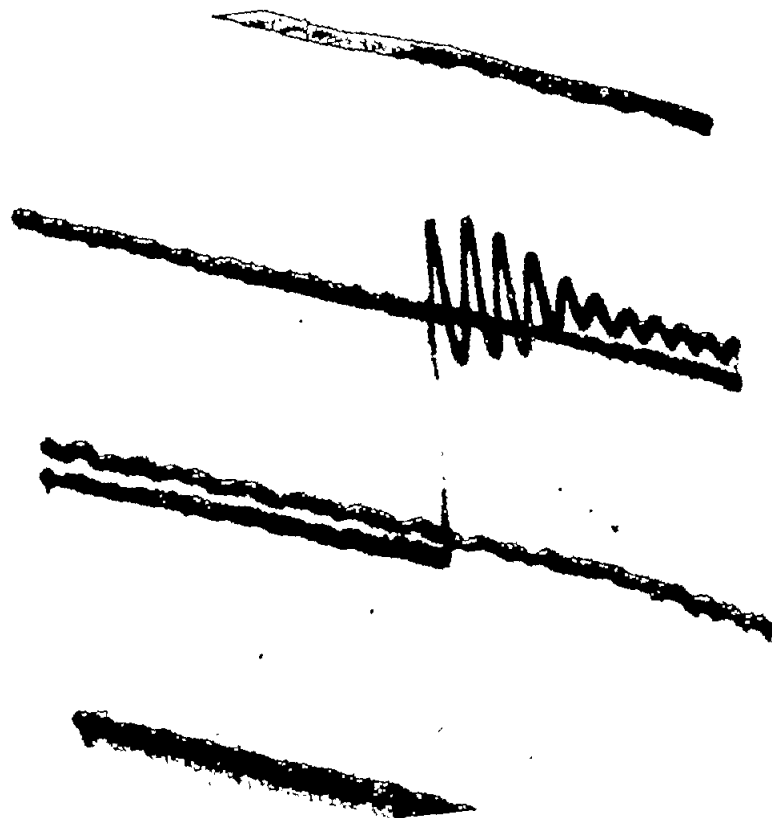
Figure 21.- Transient response of 18-millimeter strain-gage indicator taken with 2,000-cycle-per-second sweep frequency.
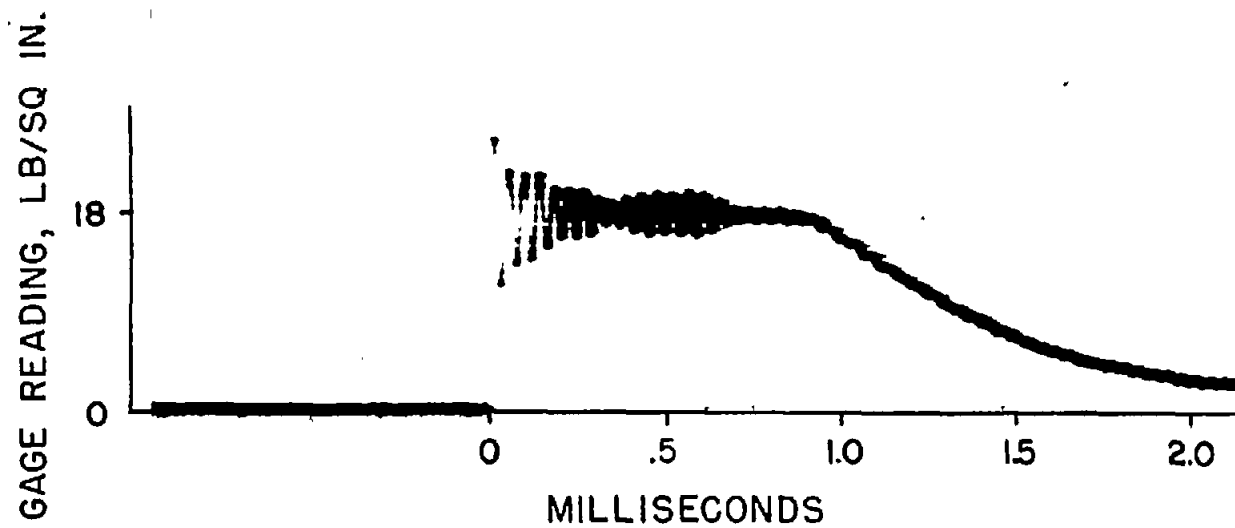
Figure 22.- Transient response of low-pressure strain-gage pickup.
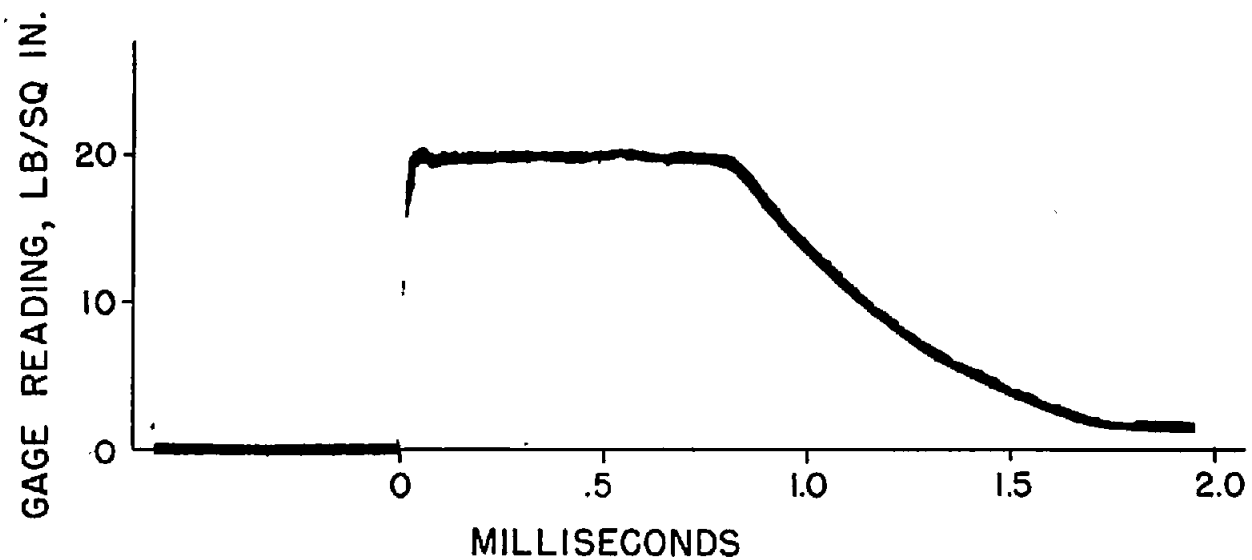
Figure 23.- Transient response of a 5/16-inch spherical-diaphragm capacitance-type indicator.
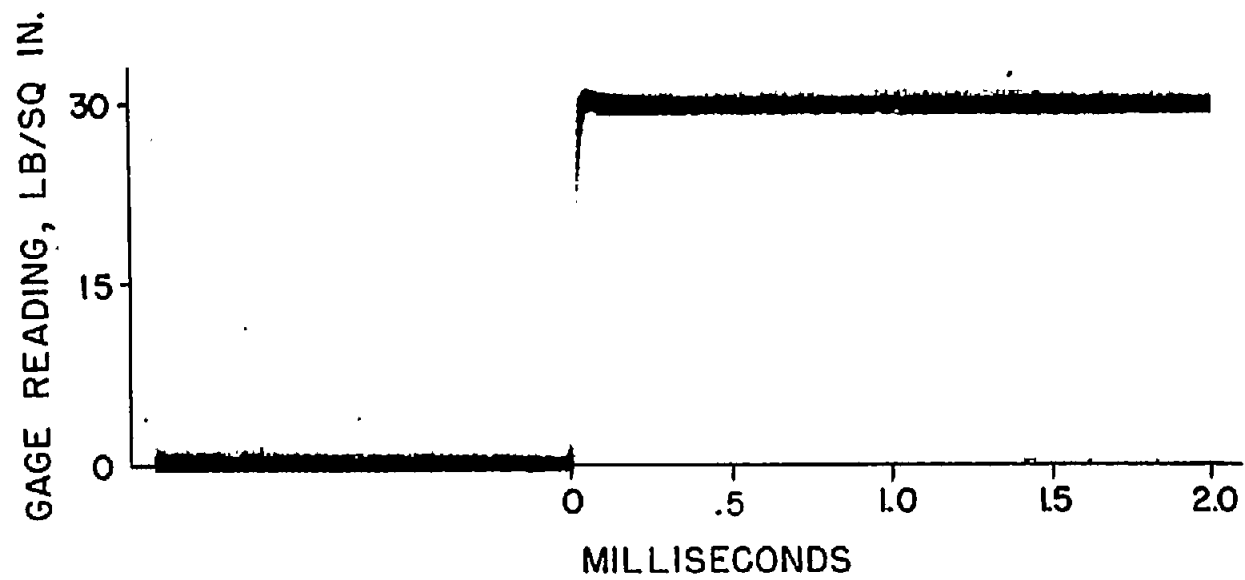
Figure 24.- Transient response of electronic systems used with spherical-diaphragm indicator.
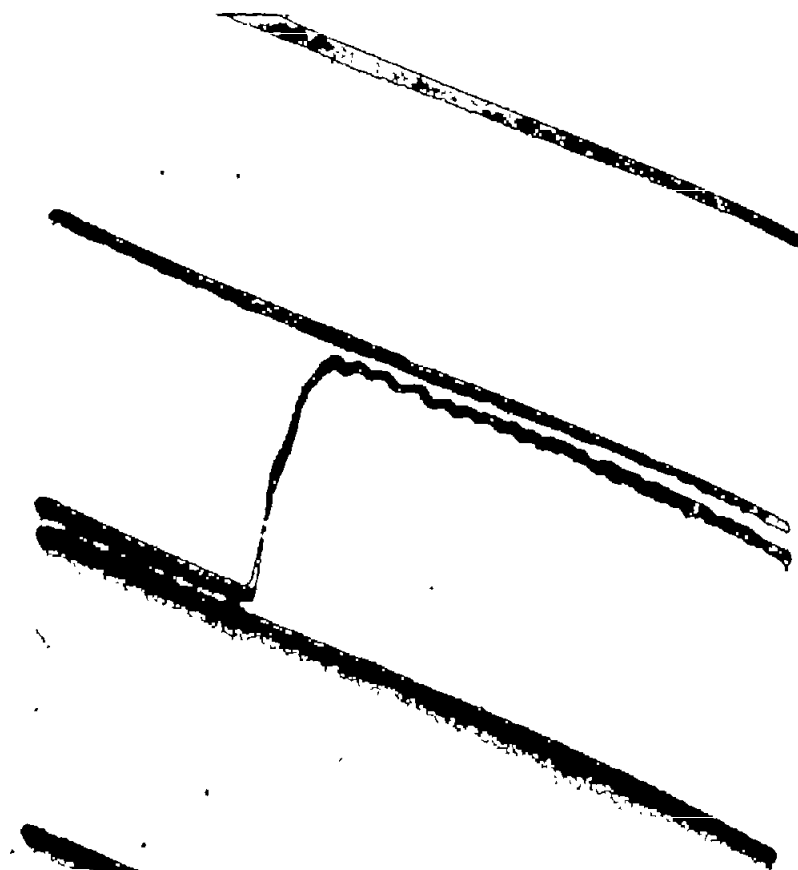
Figure 25.- Transient response of a spherical-diaphragm pressure indicator
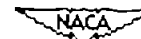with an expanded time scale taken with 2,000-cycle-per-second sweep
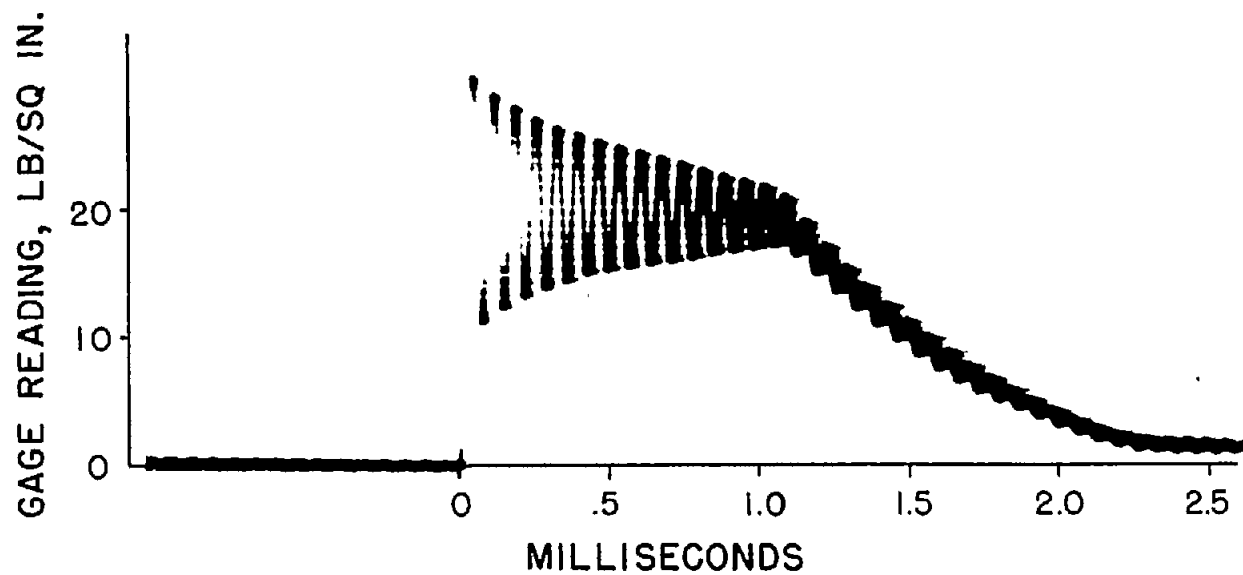frequency.

Figure 26.- Transient response of 1/2-inch flat-diaphragm indicator with
sensitivity similar to that of spherical-diaphragm indicator of figure 21.